Plasmon-Resonant Nanoparticles for Biological Imaging (and Biophotonics)

Alexander Wei
Dept. of Chemistry
Purdue University
West Lafayette, IN

2012 NanoBiophotonics Summer School
Univ. Illinois – Urbana-Champaign

Outline

I. **Plasmon resonance: physical principles and some structure-function relationships**

II. **Surface chemistry issues**

III. **Plasmon-resonant nanoparticles for biosensor applications**

IV. **Biological imaging and theranostics (photothermal applications)**

Wei, Q.; Wei, A. “Signal Generation with Gold Nanoparticles: Photophysical Properties for Sensor and Imaging Applications.” In *Supramolecular Chemistry of Organic–Inorganic Hybrid Materials* (Rurack, K., Martinez-Mañez, R. eds.) Wiley: New York, 2010; pp. 319-349
http://dl.dropbox.com/u/17739705/Wei_gold_nanoparticles_Ch10.pdf

Wei, A. “Plasmonic Nanomaterials.” In *Nanoparticles: Building Blocks for Nanotechnology* (Rotello, V. M., ed.) Kluwer: New York, 2004; pp. 173-200.
http://dl.dropbox.com/u/17739705/Wei_Plasmonic_Nanomaterials.pdf

I. Plasmon-resonant nanoparticles

Surface plasmon (SP): collective excitation of conduction electrons, using light at a resonant (visible to NIR) frequency

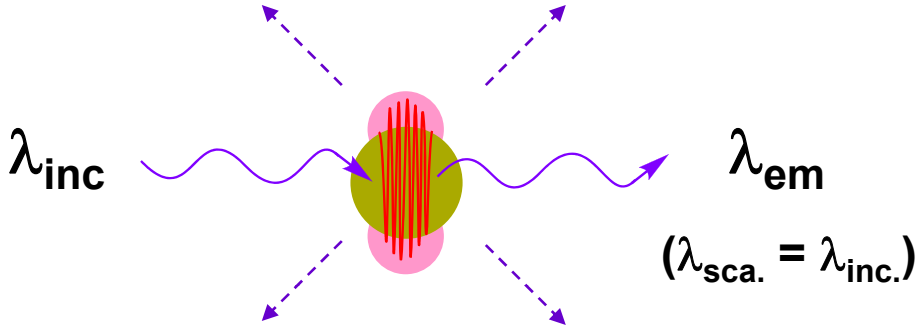

Scattering from single Au nanospheres

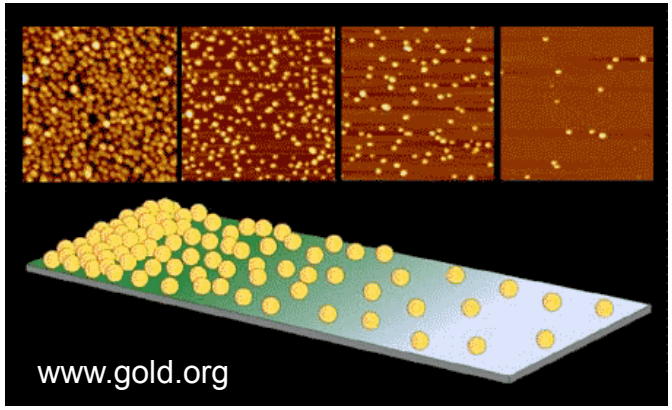

Lycurgus Cup, 4th century A.D.
British Museum, London
(Ag-Au NP's embedded in glass)

Absorption: red **Scattering: green**

Plasmon-enhanced extinctions:

$\varepsilon = 10^{9}–10^{11}\ M^{-1}\ cm^{-1}$
$C_{sca} = 10^{-13}–10^{-9}\ cm^{2}$
$\phi_{sca} = 0.04–0.90$

Ag NPs (20–150 nm):
$\lambda_{SP} = 380–600$ nm

Au NPs (20–150 nm):
$\lambda_{SP} = 520–660$ nm

Manifestations of Surface Plasmons

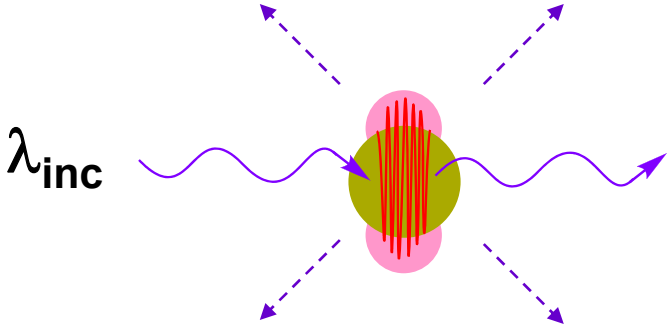

I. Localized surface plasmon resonance in metal nanoparticles ($d<\lambda_p$)

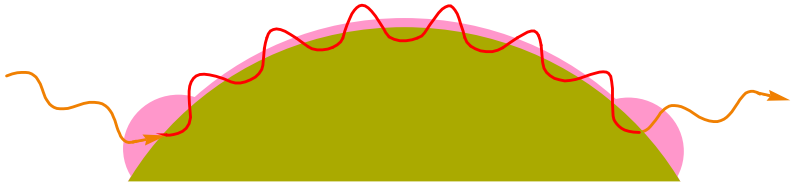

II. Surface plasmon waves (polaritons) propagating along smooth metal surface ($d>\lambda_p$)

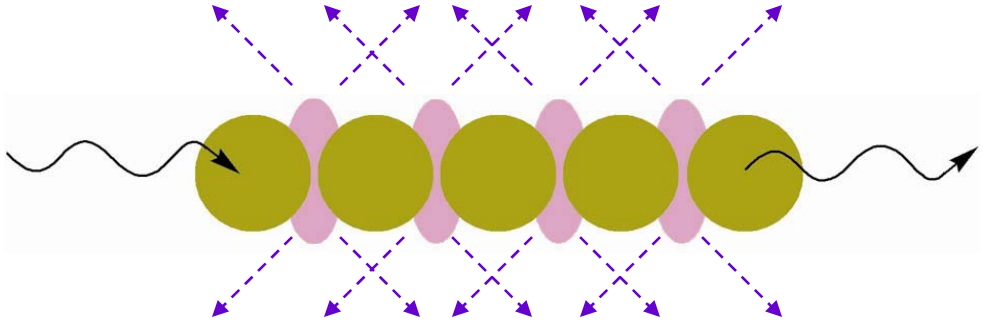

III. Coupled plasmons in nanoparticle aggregate or array

For a primer on surface plasmons, see: Wei, A. *Nanoparticles: Building Blocks for Nanotechnology*, Ed. V. M. Rotello, Kluwer Academics: New York, 2004; pp. 173-200.

Physical description of localized plasmon mode

Free-electron behavior in metals: the Drude model

Polarizability or oscillator strength α defined by the Clausius-Mosotti (a.k.a. Lorentz-Lorenz) equation:

$$\alpha = 4\pi\varepsilon_0 R^3 \left| \frac{\varepsilon - \varepsilon_d}{\varepsilon + 2\varepsilon_d} \right|$$

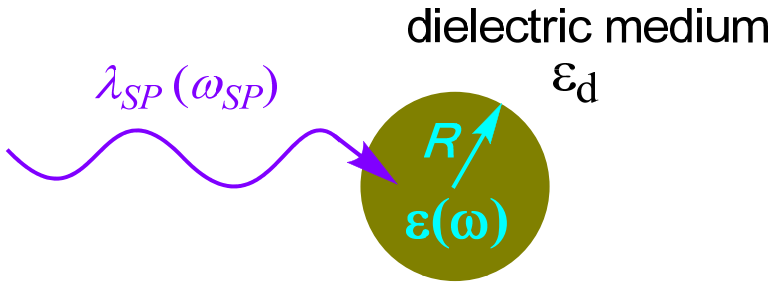

Metal NP with complex dielectric function $\varepsilon(\omega)$

Complex dielectric function $\boldsymbol{\varepsilon} = \varepsilon'(\omega) + i\varepsilon''(\omega)$;

Resonance achieved with $\varepsilon'(\omega) = -2\varepsilon_d$, $\varepsilon''(\omega) << 1$

Given a plasma frequency ω_p such that $\varepsilon(\omega_p) = 0$:

Ideally, $\omega_{SP} \approx \dfrac{\omega_p}{\sqrt{2\varepsilon_d + 1}}$

$$\varepsilon'(\omega) \approx 1 - \frac{\omega_p^2}{\omega^2 + \Gamma^2} \qquad \varepsilon''(\omega) \approx \frac{\omega_p^2 \Gamma}{\omega(\omega^2 + \Gamma^2)}$$

However, free-electron response is coupled with interband transitions (e.g., Au(5*d*→6*s*)), which changes ω_{SP}

where Γ is the plasma relaxation frequency.

Only metals with low $\varepsilon''(\omega)$ at ω_{SP} will exhibit strong plasmon resonance: **Ag > Au > Cu**

Physical description of plasmons (cont'd)

Electrodynamic Mie Theory

Can calculate dipolar optical response with great accuracy, especially if performed under "quasi-static" conditions (valid when particle size is less than 30 nm)

Generalized Mie Theory:

Can calculate approximate optical response for metal nanoparticles of all shapes and sizes; accounts for higher-order effects such as phase retardation, quadrupolar resonances, etc.

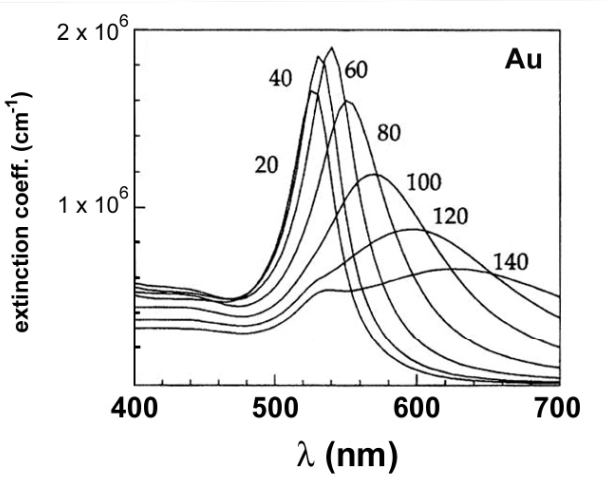

Calculated plasmon response from spherical Au nanoparticles in H_2O:

Yguerabide, *Anal. Biochem.* **1998**, *262*, 137.

eV-to-λ (nm) conversion: $\lambda = \frac{1239}{\text{eV}}$

Calculated response (extinction) from metal nanoparticles (in air):

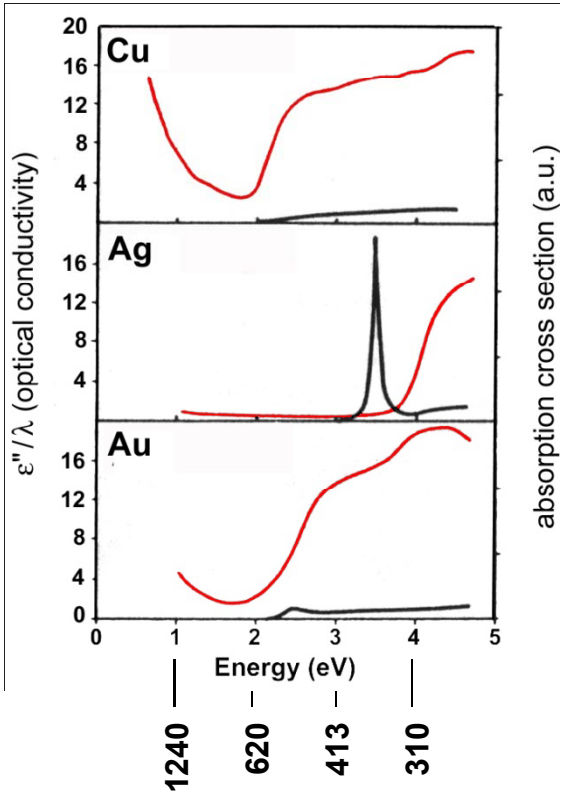

Kriebig and Vollmer, *Optical Properties of Metal Clusters, c.*1995.

Size effects on plasmon resonance

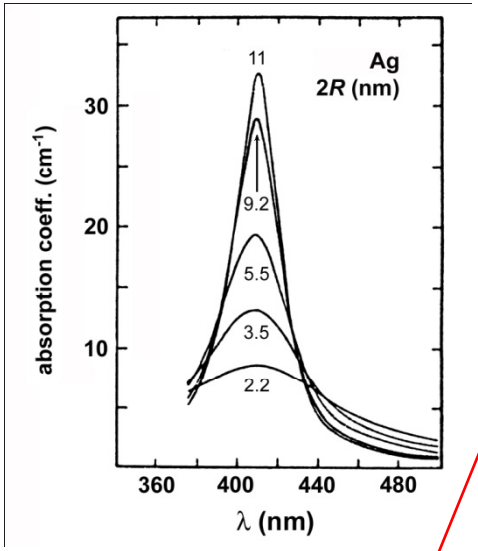

Surface scattering of oscillating electrons: plasmon lineshape (Γ) broadens with $1/R$

Phase retardation: redshift and broadening of λ_{SP} for particles greater than L_E, the electron mean free path (40-50 nm)

Higher-order plasmon resonances: increase in probability with larger particle size (also a function of L_E)

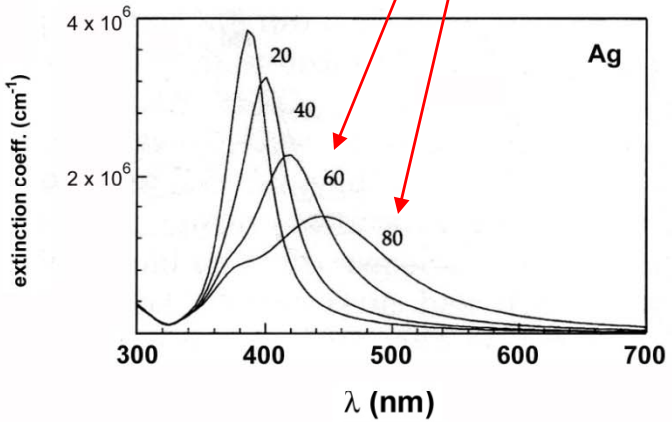

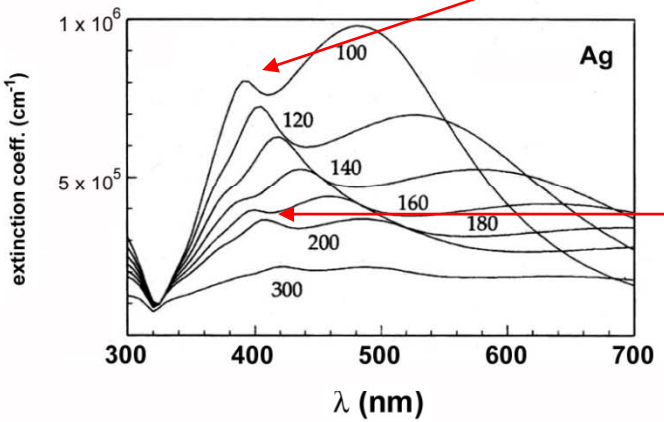

Dipolar mode

Quadrupolar mode

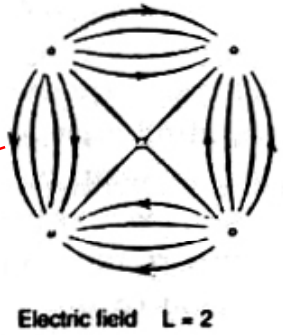

Octupolar mode

Calculated plasmon response from spherical Ag nanoparticles in H_2O: Yguerabide, *Anal. Biochem*. **1998**, *262*, 137.

Dielectric (medium) effects on plasmon resonance

LSPRs and FWHM linewidths of Ag nanoparticles in different environments (calculated)

Kriebig and Vollmer, *Optical Properties of Metal Clusters, c.*1995.

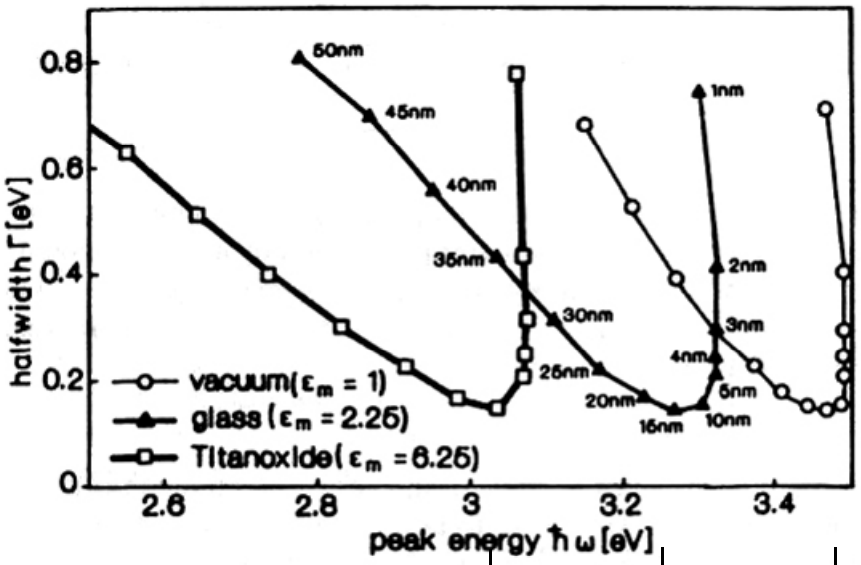

413 nm 387 nm 364 nm

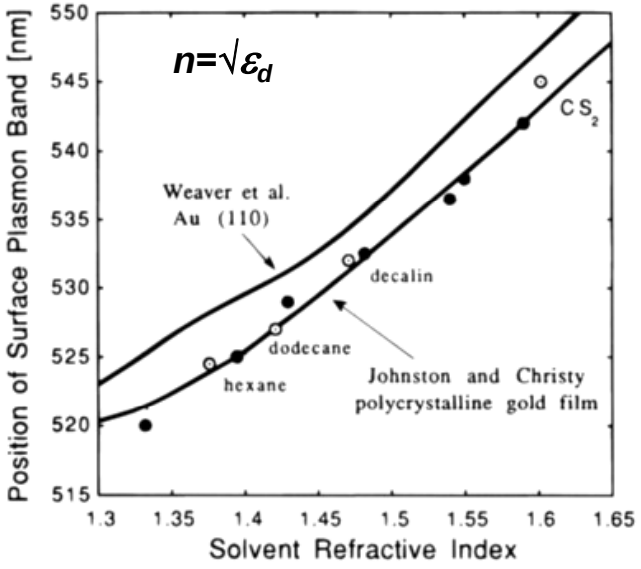

Solvatochromatism in polymer-stabilized Au nanoparticles

Underwood and Mulvaney, *Langmuir* **1994**, *10,* 3427.

Effect of shape anisotropy: Au nanorods

Au NRs: Tunable resonances in the NIR

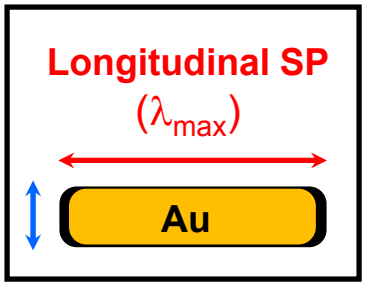

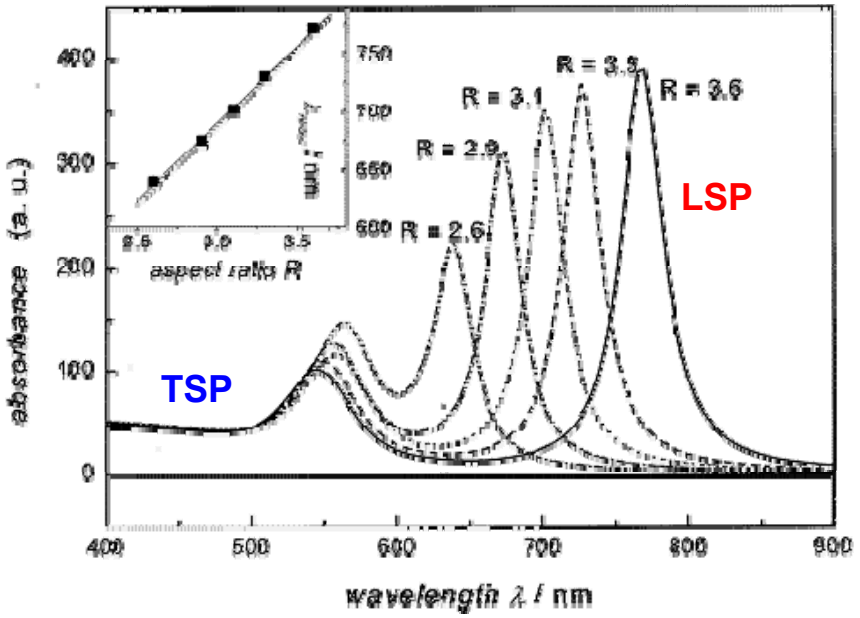

***SP modes as a function of aspect ratio*:**
Link and El-Sayed, *J. Phys. Chem. B* **1999**, *103*, 3073

"Biological window" in tissue at NIR wavelengths:

Attenuation is minimized between 750 nm and 1.3 *μ*m

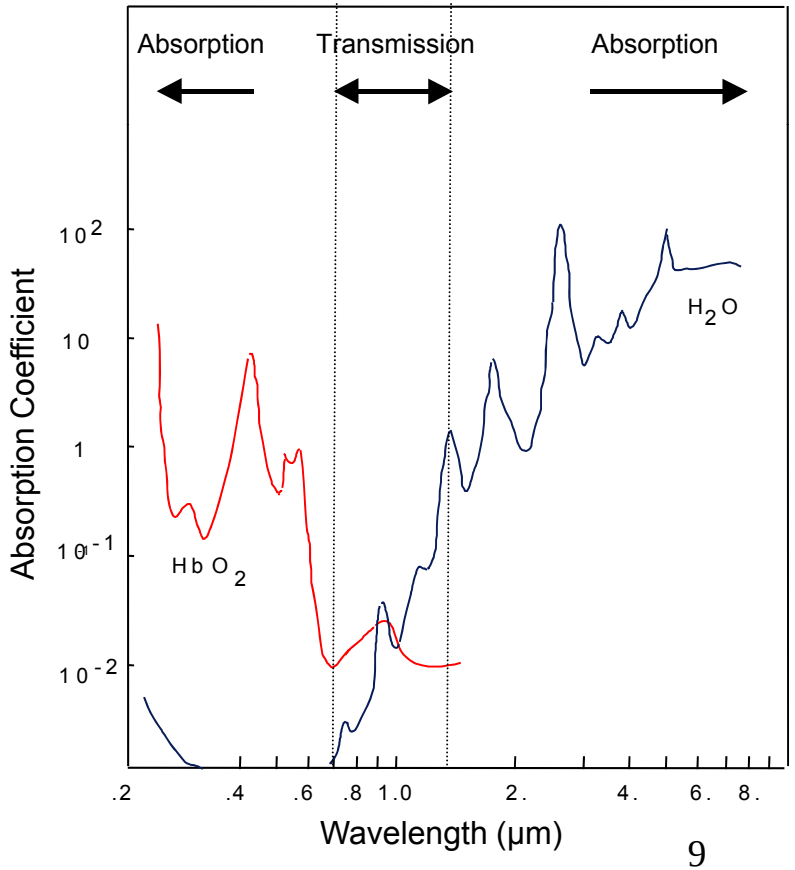

Other anisotropic Au nanoparticles

Nanoprisms (by nanosphere lithography)

Haynes and van Duyne, *J. Phys. Chem. B* **2001**, *105*, 5599.

Kelly et al, *J. Phys. Chem. B* **2003**, *107*, 668

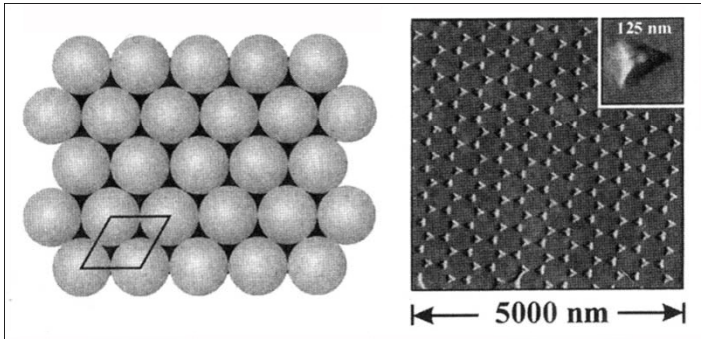

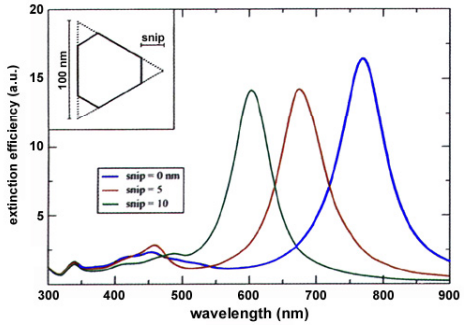

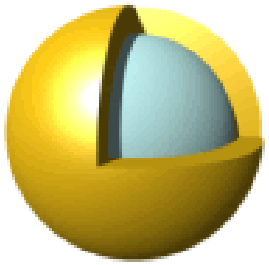

Nanoshells (SiO_2@Au)

Lal et al., *Acc. Chem. Res.* **2008**, *41*, 1842

Pentagonal bipyramids (decahedra)

Sanchez-Igleisias et al, *Adv. Mater.* **2006**, *18*, 2529

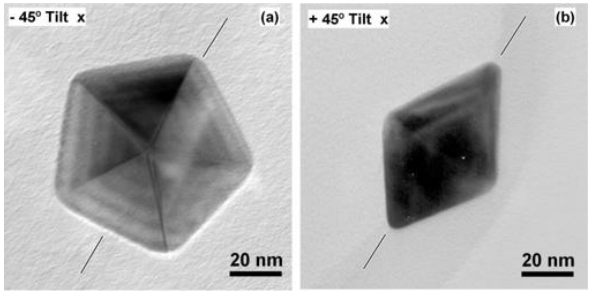

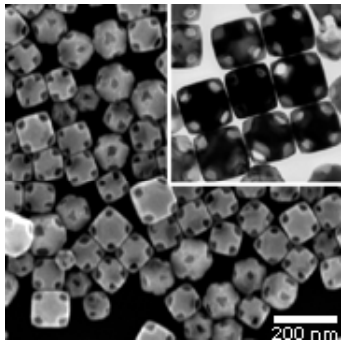

Nanocages (growth on Ag nanocubes, with galvanic displacement)

Siekkinen et al, *J. Am. Chem. Soc.* **2006**, *128*, 14776

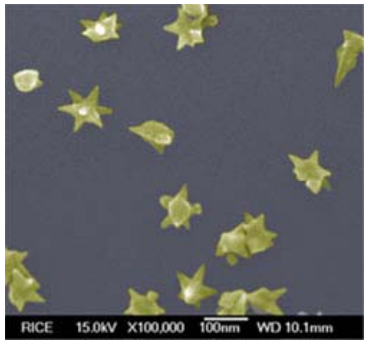

Nanostars (seeded growth from Au NPs)

Nehl, Liao, and Hafner, *Nano Lett.* **2006**, *6*, 683

II. Surface Functionalization

Nonspecific (protein) adsorption and cell uptake: a constant problem

<u>Key stability issues</u>:

- Dispersion control (entropic steric repulsion; electrostatic stabilization)

- Robustness (adhesion)

<u>Surface coating methodologies</u>:

A. Physical adsorption (physisorption)

B. Chemical adsorption (chemisorption)

C. Core-shell growth

D. Polymer brush growth

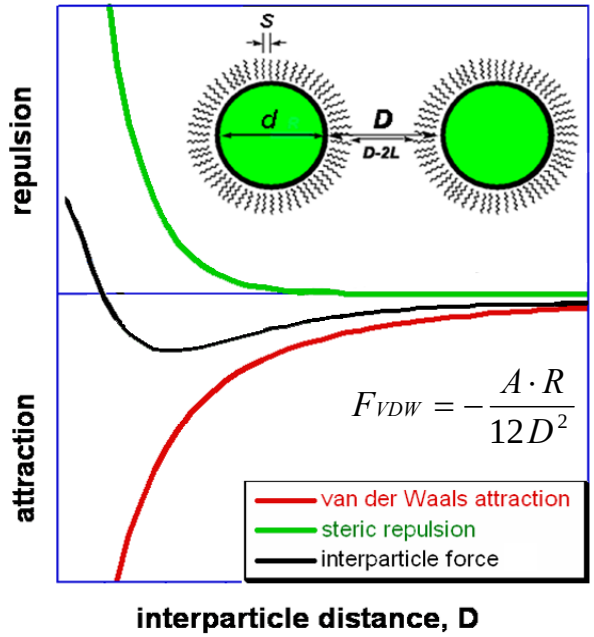

Wei, *Chem Commun.* **2006**, 1581.

A. Physisorptive coatings

Electrostatic adsorption: proteins, polyelectrolytes

Hayat, *Colloidal Gold: Principles, Methods, and Applications*; Academic Press: San Diego, 1989.

Layer-by-layer (LbL) adsorption: multilayer polyelectrolyte coating with nanometer control

Quinn et al, *Chem. Soc. Rev.*, **2007**, *36*, 707.

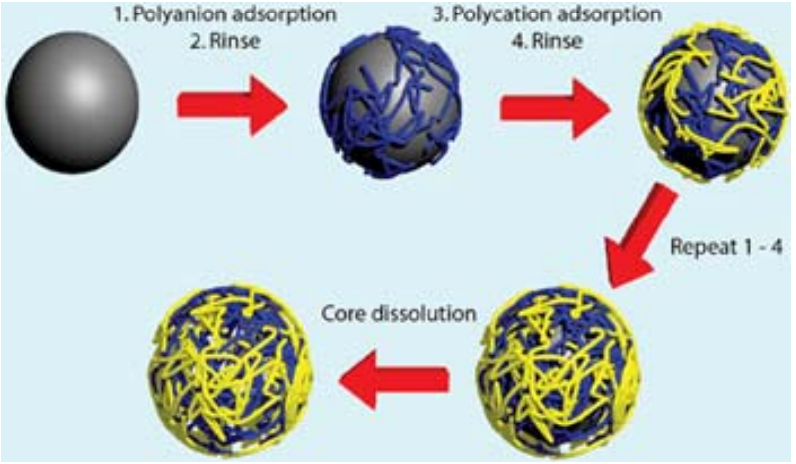

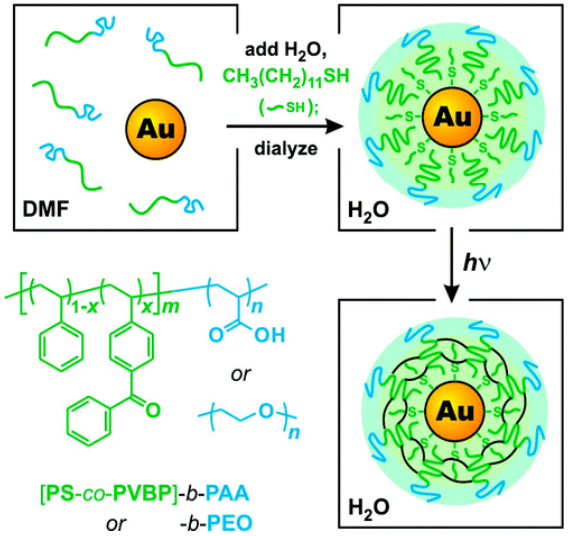

Surfactants (surface-active agents)

Hydrophobic self-assembly; stabilization by crosslinking (core-shell formation)

Chen, Cho, Young, and Taton, *Langmuir* **2007**, *23*, 7491

B. Chemisorptive coatings

Self-assembled monolayers (SAMs) based on alkylthiols

Monolayer-protected Au clusters (MPCs)

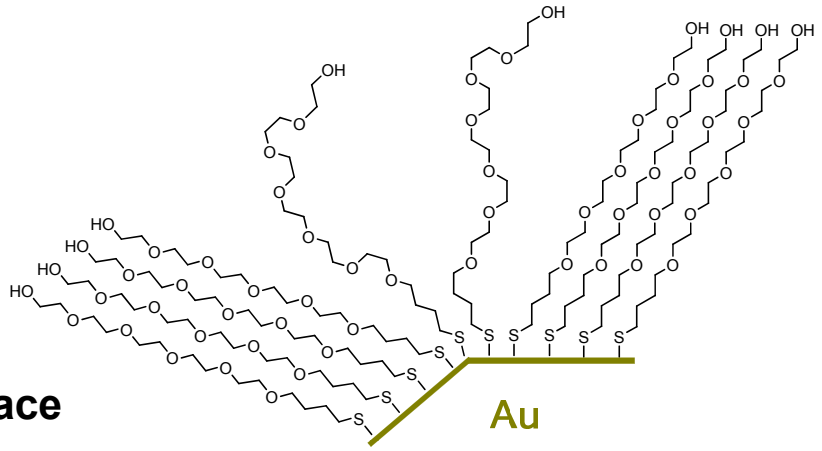

Ex. thiol-immobilized PEG on Au NP surface

Concern: Thiols can be oxidized and displaced from Au surfaces by other thiols, such as free cysteine (blood) or glutathione (intracellular).

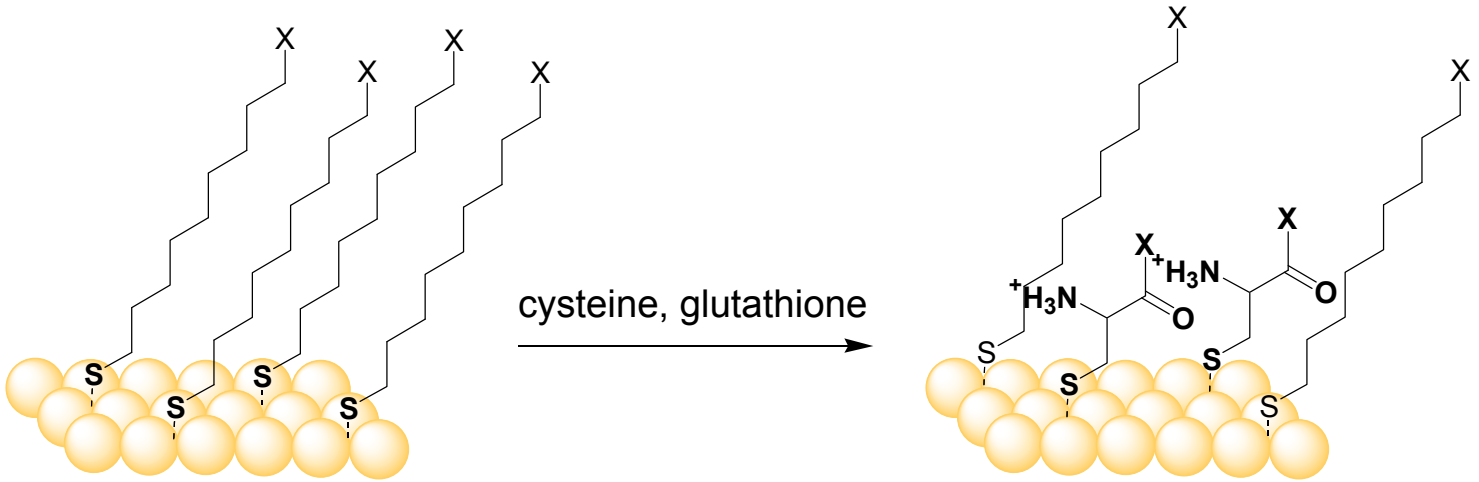

Au nanoprobe surface

deterioration of surface

in situ Dithiocarbamate (DTC) formation: Chemisorptive alternative to thiols

alkylamines **DTC ligands**

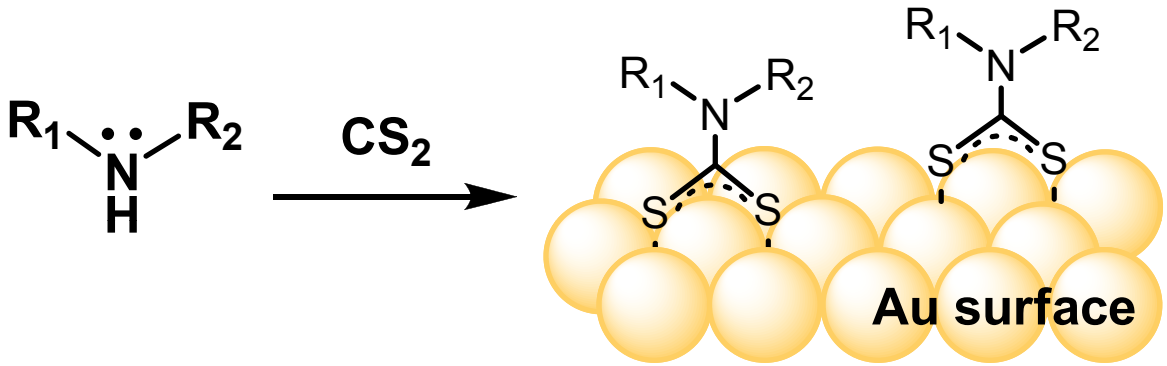

Examples:

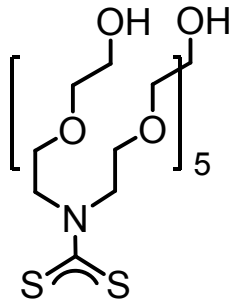

oligoethylene glycols (OEG)

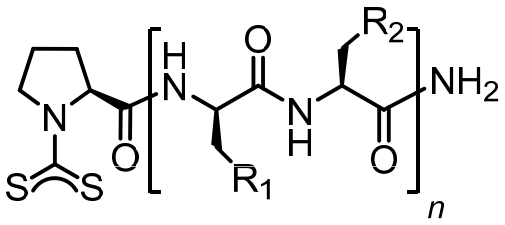

oligopeptides

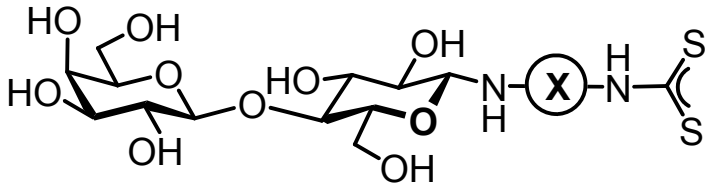

carbohydrates

Zhao, Pérez-Segarra, Shi, and Wei, *J. Am. Chem. Soc*. **2005**, *127*, 7328.
Zhu et al. *Langmuir* **2008**, *24*, 8660.

Targeting cell membrane receptors with ligand-functionalized Au nanorods

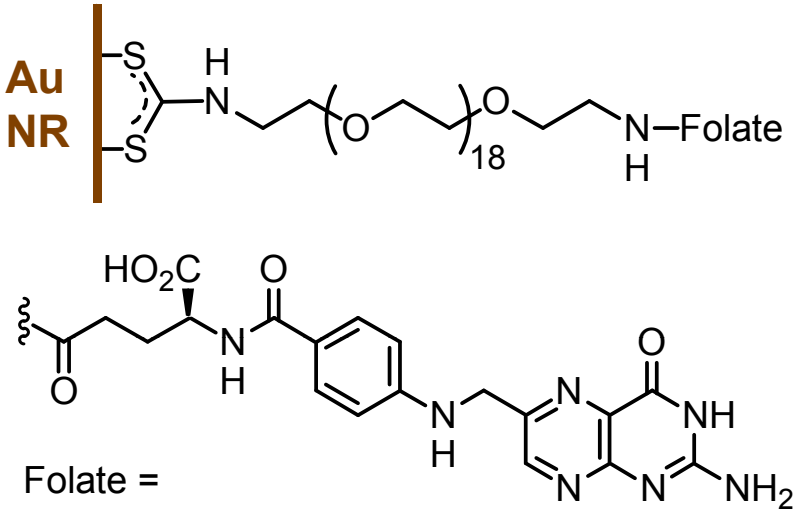

Folate–oligoethyleneglycol ligands conjugated onto nanorod surfaces by *in situ* DTC assembly

Slower rates observed for receptor-mediated nanorod uptake

Tong et al.. *Adv. Mater*. **2007** *19*, 3136.

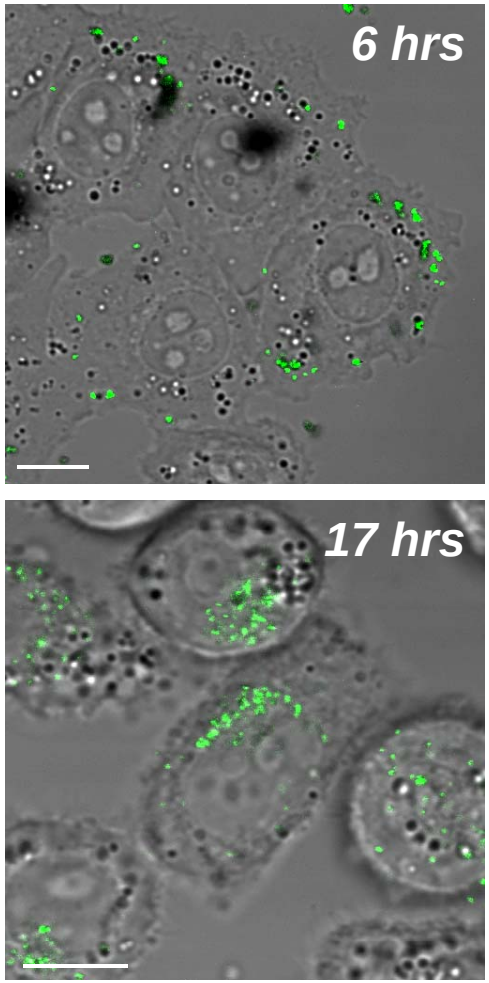

C. Core-shell nanoparticles (examples)

1. Silica coating

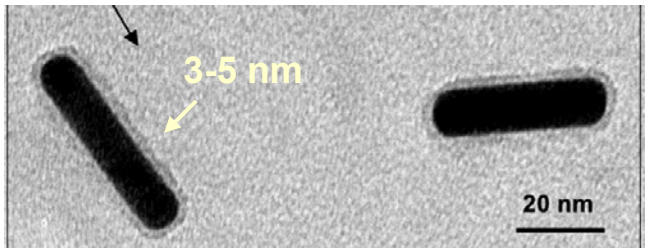

Sendroiu, Warner, and Corn,
Langmuir **2009**, *25*, 11282.

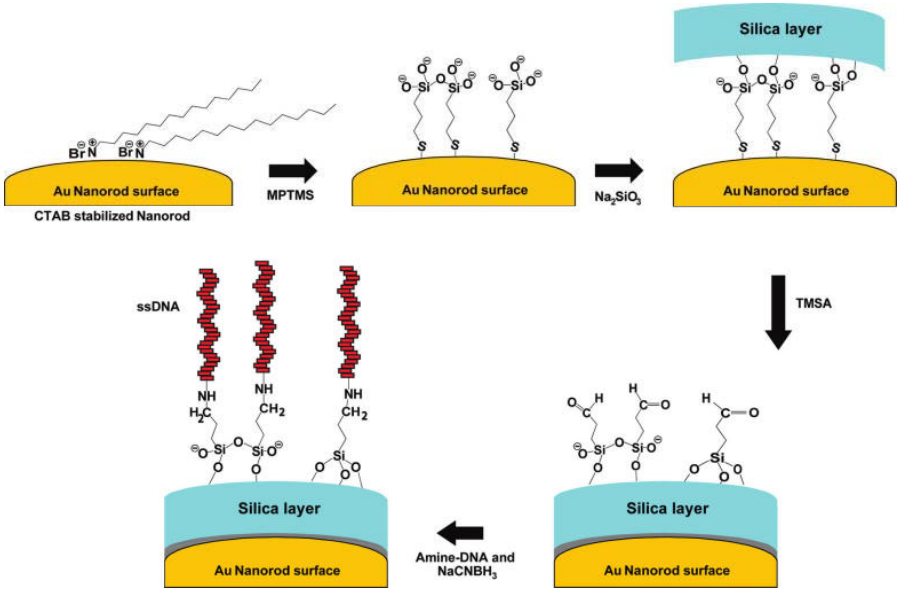

2. Emulsion polymerization

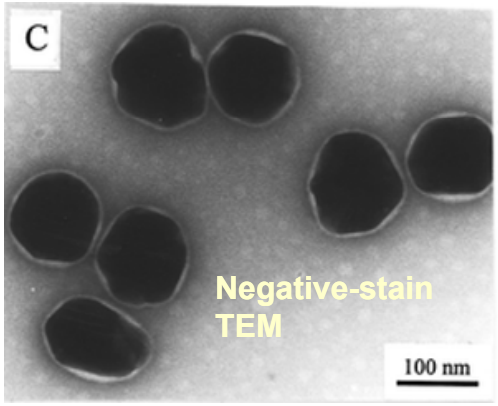

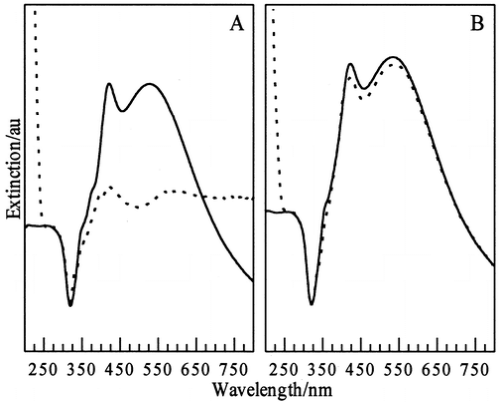

A. Corrosion of uncoated Ag nanoparticles in 1.8 M NaCl, after 1 hr.

B. No corrosion for polymer-coated NPs.

Quaroni and Chumanov, *J. Am. Chem. Soc.* **1999**, *121*, 10642.

D. Polymer brush coatings

Radial, core-shell growth vs. surface-limited "grafting"

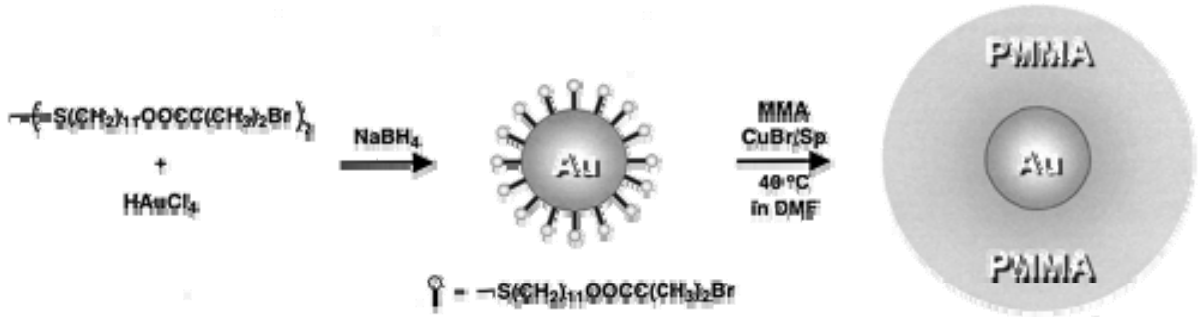

Ohno, Koh, Tsuji, and Fukuda, *Macromolecules* **2002**, *35*, 8989.

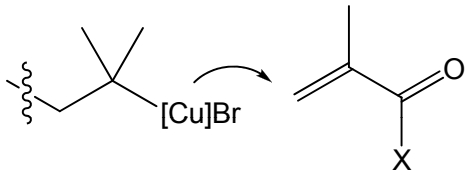

Atom-trap radical polymerization (ATRP): "living" polymer brush growth
Excellent control over thickness, surface properties

Bestows additional function for drug delivery applications (e.g., thermoresponsive volume changes, coupled to photothermal effects)

Poly(N-isopropyl)acrylamide (pNIPAM);

Lower critical solution transition (LCST) temperature ca. 32 °C

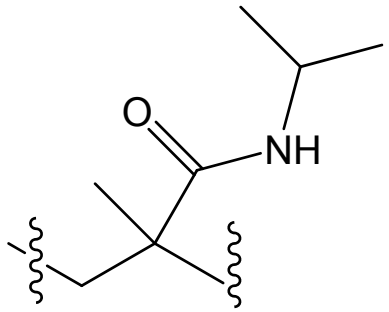

Raula et al., *Langmuir* **2003**, *19*, 3499.
Kawano et al., *Bioconjug. Chem.* **2009**, *20*, 209.

III. Optical biosensor applications

A. Resonant light scattering (nanoparticles as labels)

Size-dependent color response (Au NPs):

<50 nm: λ_{SPR}= 520-530 nm (green)

80 nm: λ_{SPR}= 560-570 nm (yellow)

100+ nm: λ_{SPR}= 580+ nm (orange)

Detection of DNA hybridization by darkfield (scattering) microscopy:

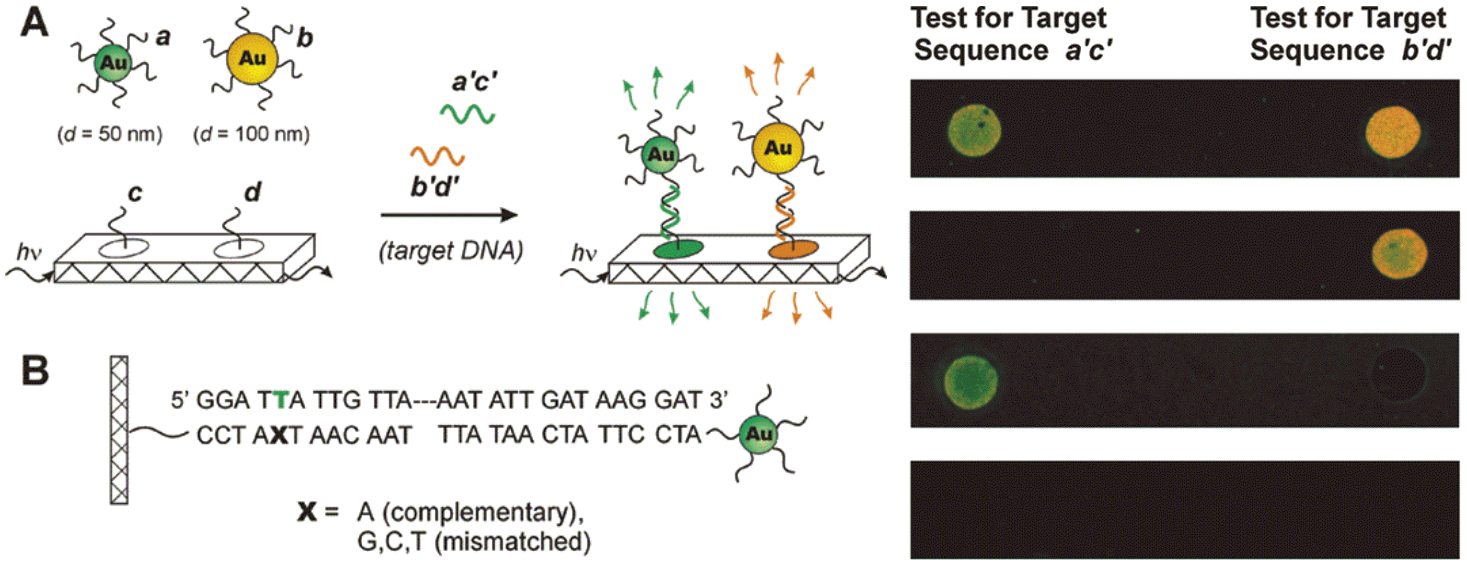

Taton, Lu, and Mirkin, *J. Am. Chem. Soc.* **2001**, *123*, 5164.

Aggregation-induced amplification of light scattering

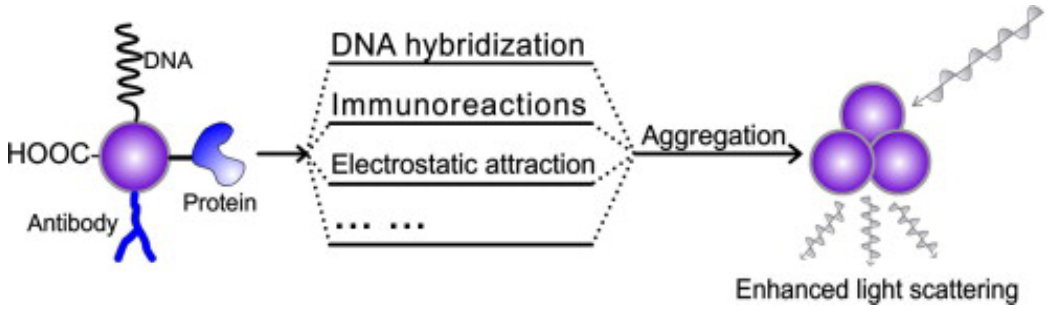

Ling et al, *Trends Anal. Chem.* **2009**, *28*, 447.

DNA-induced aggregation of 30-nm Au NPs monitored by dynamic light scattering (DLS)

low picomolar (pM) resolution;
sensitive to base-pair mismatches

Dai et al, *J. Am. Chem. Soc.* **2008**, *130*, 8138.

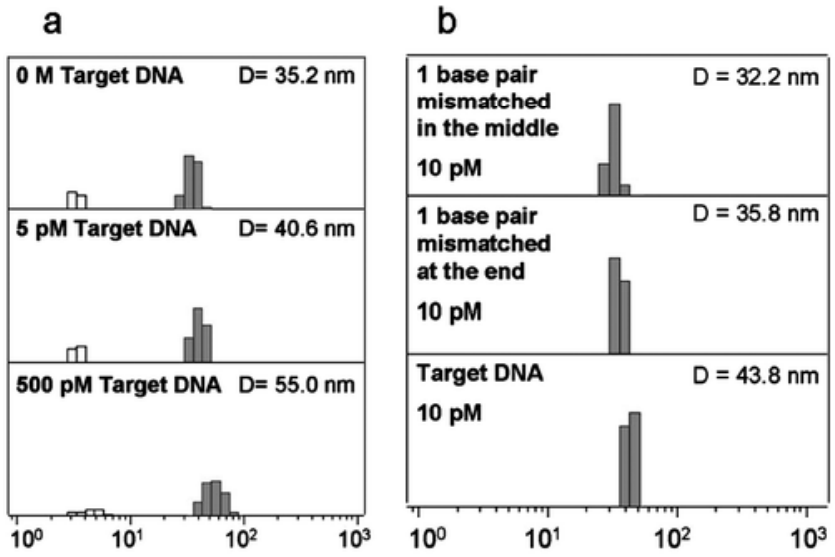

B. Colorimetric assays

Analyte-dependent aggregation = plasmon resonance shift

Lectin-induced aggregation of 9-nm Au NPs, with thiol-anchored lactose (glyco-NPs):

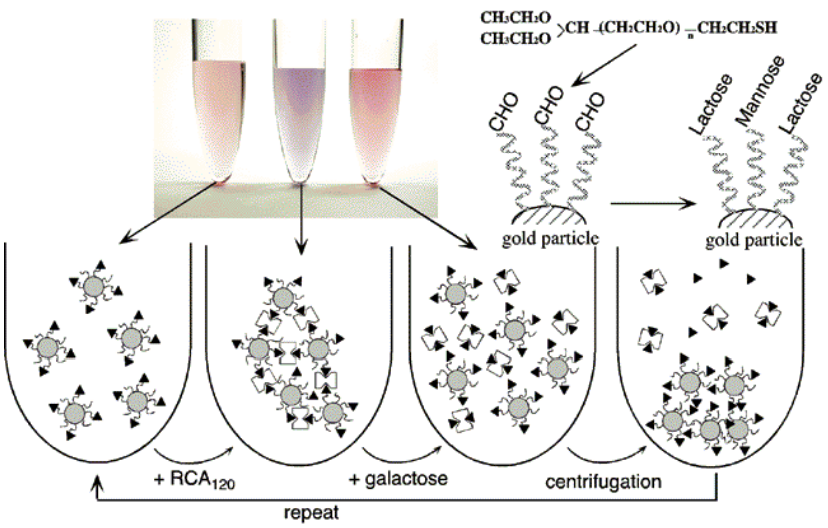

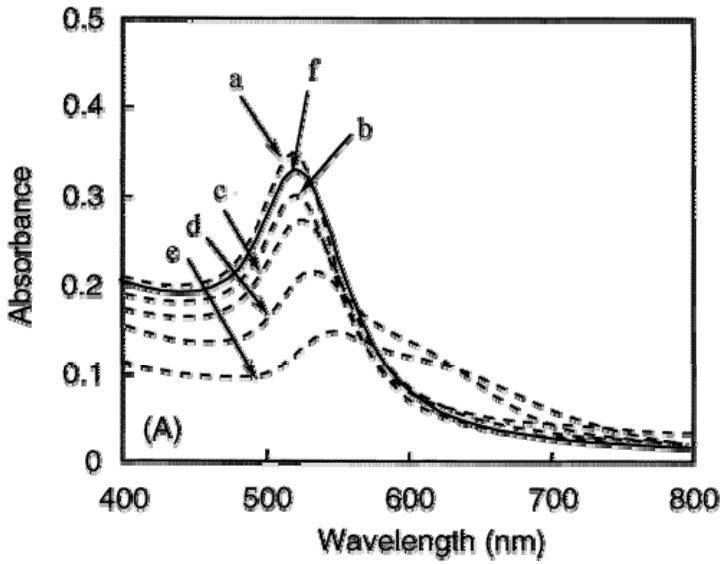

Otsuka, Akiyama, Nagasaki, and Kataoka, *J. Am. Chem. Soc.* **2001**, *123*, 8226.

After lectin addition (μg/mL): (a) 0; (b) 5; (c) 10; (d) 20; (e) 50. (solid line) redispersed NPs, after adding excess galactose.

For other examples of Au nanoparticles in colorimetric assays, see: *Inorganic Nanoprobes for Biological Sensing and Imaging*, Eds. H. Mattoussi, J. Cheon, Artech House:New York, 2009; Chapter 8 (Rotello and coworkers)

C. Localized surface plasmon resonance

Changes in surface dielectric = plasmon resonance shift

Single-nanoparticle SPR spectroscopy

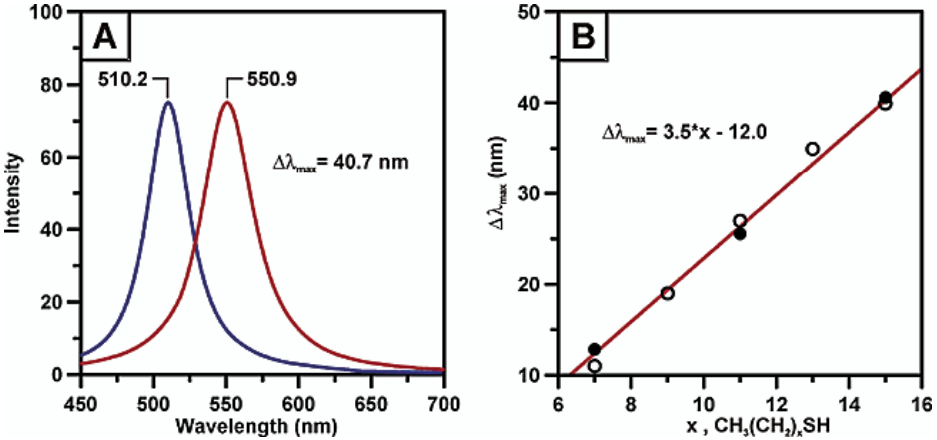

(A) Ag NP before and after adsorption of C16-thiol.
(B) LSPR response vs. thiol chain length.

Anisotropic nanoparticles are more sensitive to local changes in surface dielectric; measured in refractive index units (RIU)

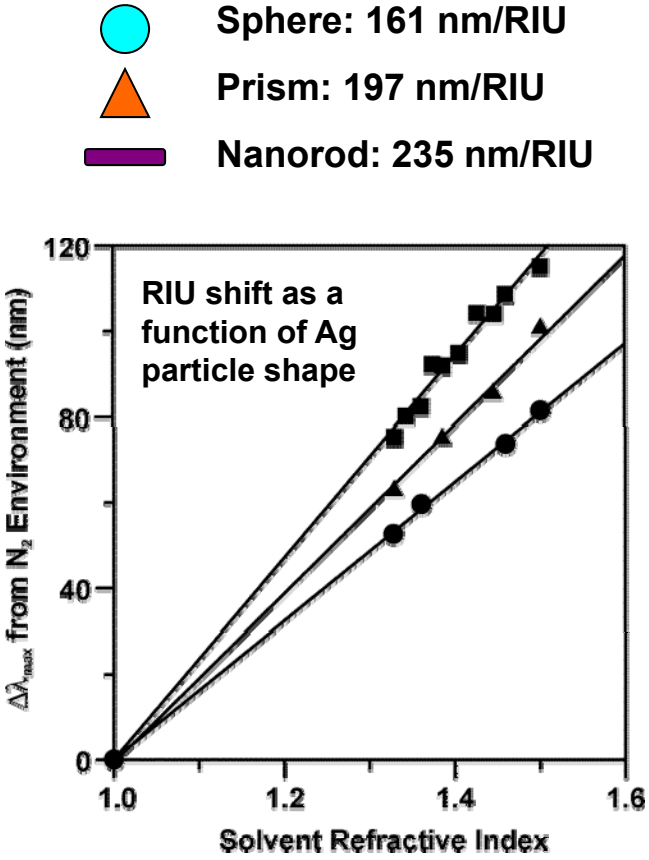

McFarland and van Duyne, *Nano Lett*. **2003**, *3*, 1057.

Examples of LSPR biosensing

Antibody-labeled Au nanorods for multiplex biosensing

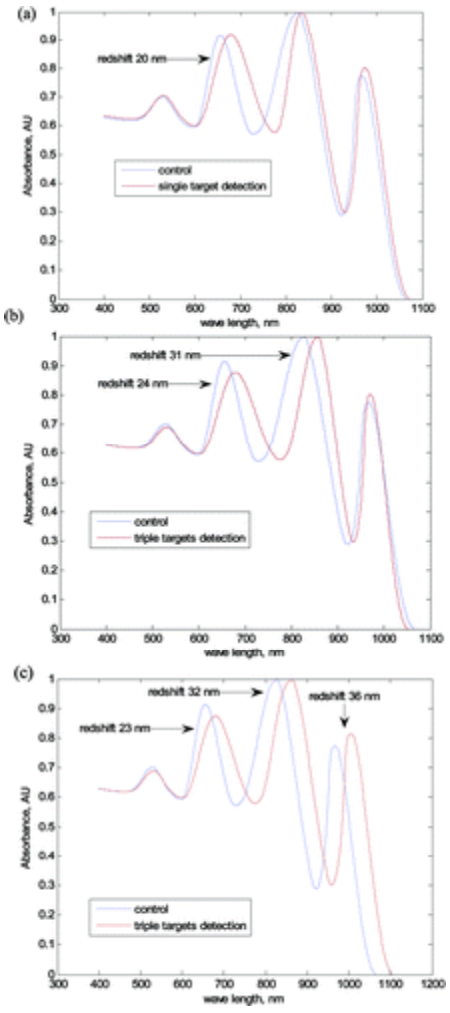

Yu and Irudayaraj, *Anal. Chem.* **2007**, *79*, 572

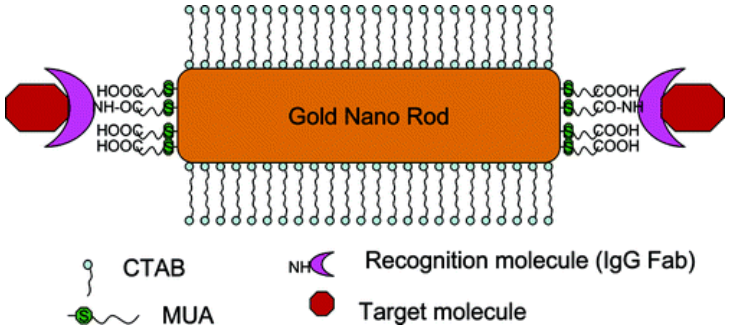

Real-time LSPR with antibody-labeled pentagonal bipyramids

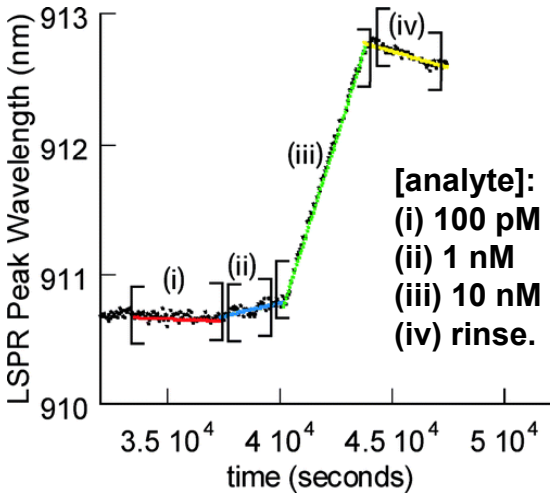

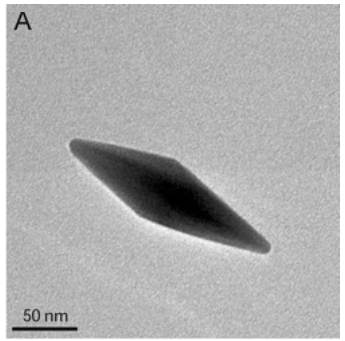

λ_{LSPR} = 750-900 nm

LSPR sensitivity: 280-380 nm/RIU

Lee, Mayer, Hafner, *Anal. Chem.* **2009**, *81*, 4450.

D. Plasmon-enhanced emissions

Plasmon-amplified signals in surface-enhanced Raman scattering (SERS) and other optical emissions are based on <u>local field effects</u>

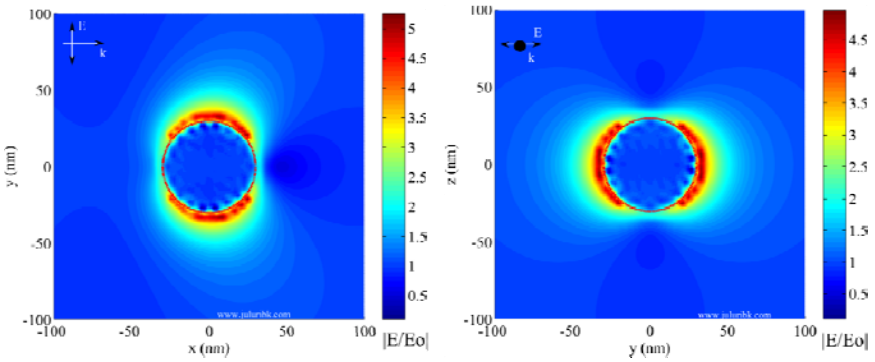

Local EM field factors (E/E_0):
extends for several nanometers from NP surface, in direction of LSPR mode

Calculation of $G = (E/E_0)^4$ in Ag NP dimer, as a function of interparticle separation

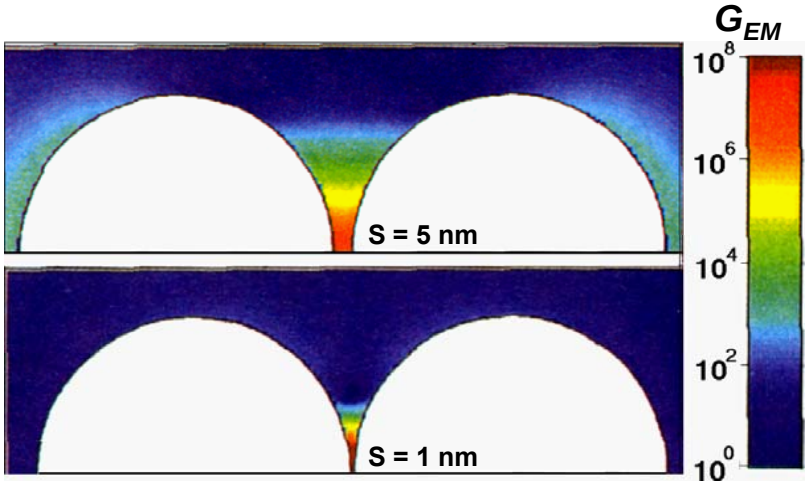

λ_{ex}=514.5 nm; *2R* =90 nm, S= 1 or 5 nm (Ag)
Xu et al, *Phys. Rev. E* **2000**, *62*, 4318.

EM field factors in NP assemblies:

Local EM field factors increase nonlinearly with decreased spacing between NPs; field factors are typically highly localized

Size of ensemble, unit particle size are also important factors in EM enhancement

Surface-enhanced Raman scattering (SERS)

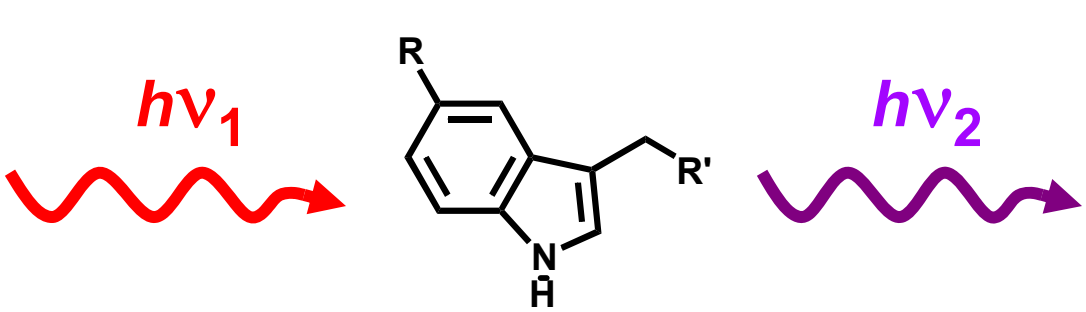

analyte

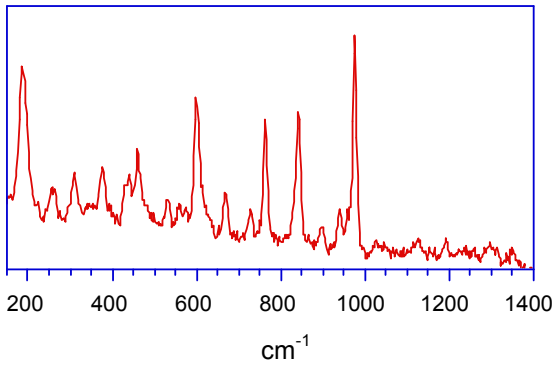

Raman spectrum

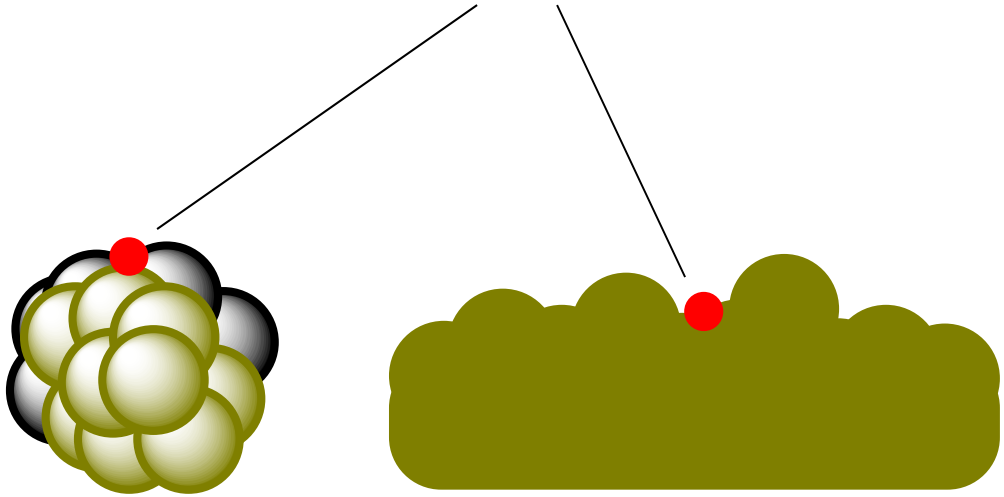

nanostructured Ag and Au surfaces (roughness ~ 10-200 nm)

- Label-free chemical sensing
- Multiplexing capabilities
- Water is Raman-silent
- relationship between nanostructure and activity often not well-defined
- SERS-active substrates are easy to make, but can be tricky to reproduce

“Hot Spots” in SERS-active substrates

SERS activity is strongly correlated with local electromagnetic (EM) field factors

“Hot spots” can be found at edges and tips of anisotropic NPs, but can be even stronger in gaps between closely spaced metal nanostructures

SERS-active “nano-crescents”

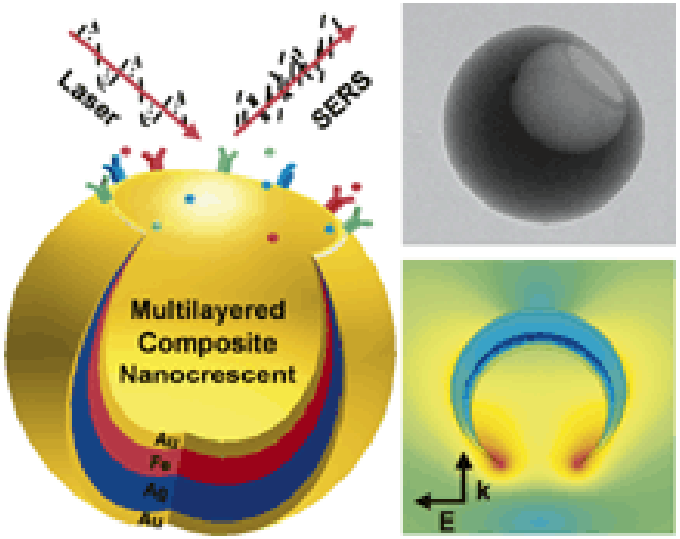

Liu et al. *Adv. Mater.* **2005**, *17*, 2683.

Au nanoparticle arrays

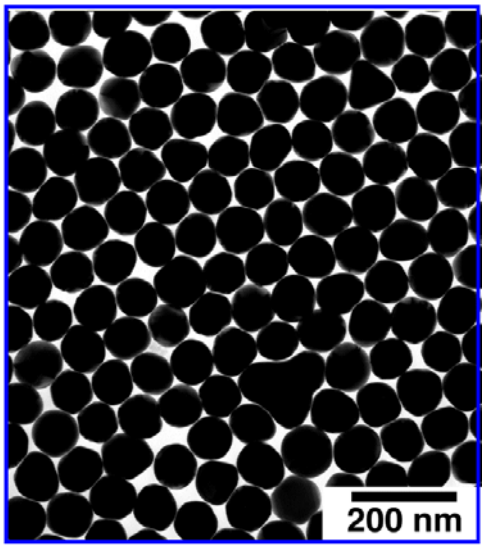

Wei et al, *ChemPhysChem* **2001**, *2*, 743.

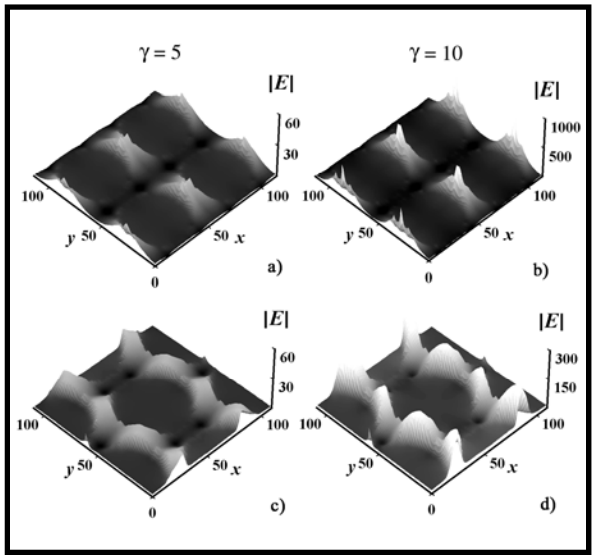

Genov, Sarychev, Shalaev, Wei, *Nano Lett.* **2004**, *4*, 153.

Surface-enhanced fluorescence (SEF)

Highly sensitive to distance between fluorophore and metal surface: SEF also relies on local EM field factors, but excited states can be quenched by back-electron transfer

Molecular spacers are important for optimizing SEF

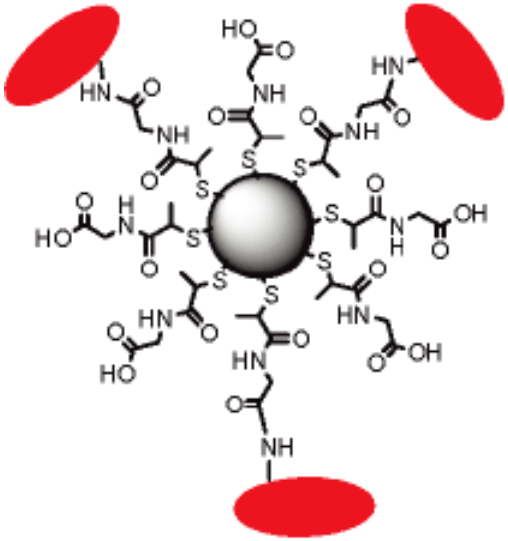

20-nm Ag NP coated with labeled lectin (ConA)

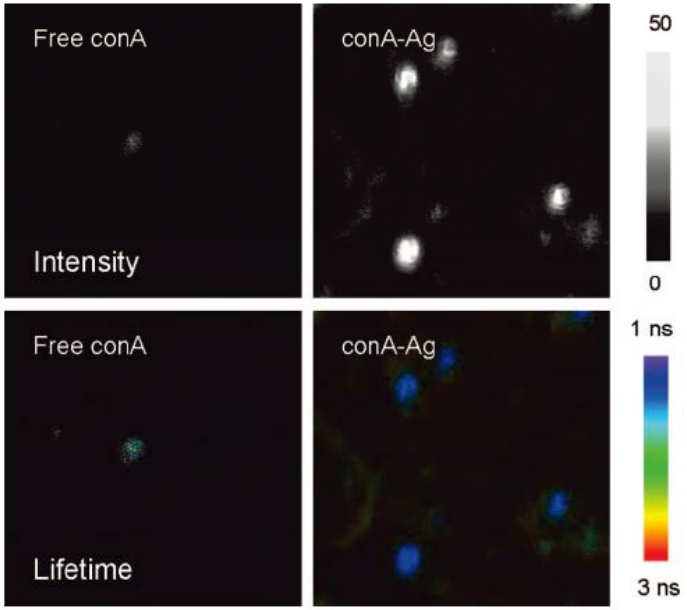

Fluorescent ConA, without and with coupling to Ag NPs

20–30-fold SEF by Ag NP core: Zhang, Fu, and Lakowicz, *Bioconjug. Chem*. **2007**, *18*, 800.

Plasmon-enhanced fluorescence lifetime imaging (FLIM): Zhang et al, *Nano Lett*. **2008**, *8*, 1179.

Förster resonance energy transfer (FRET)

Energy transfer mediated by overlap between emission and absorption (donor−acceptor) bands; D−A distance <10 nm

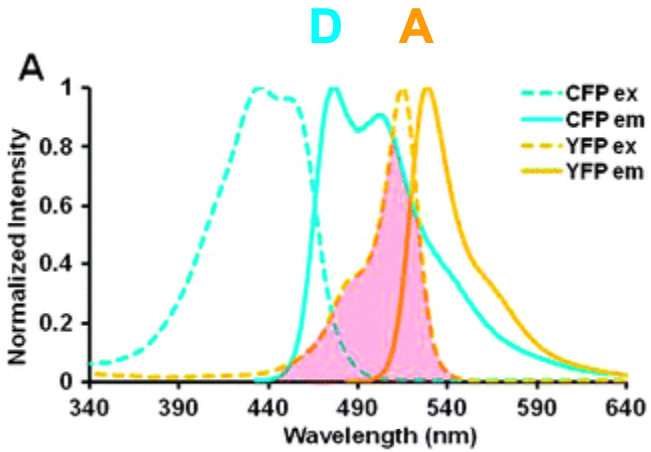

Wang and Wang, *Integr. Biol.* **2009**, *1*, 565

Plasmon-enhanced FRET: greater efficency and range

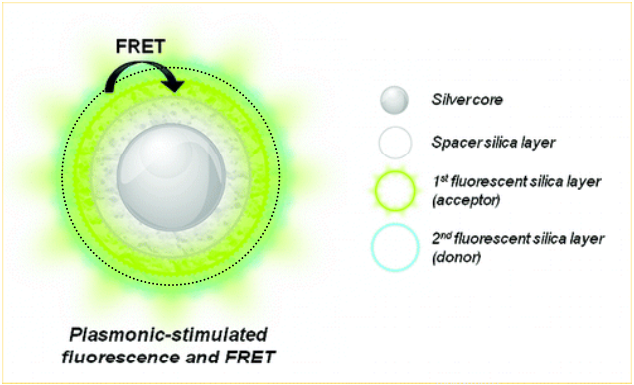

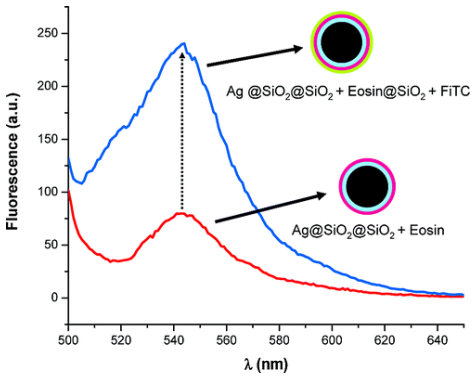

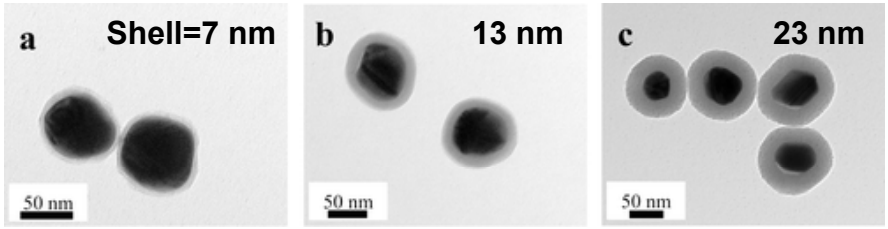

Dye-doped Ag@SiO_2 core-shell NPs

Lessard-Viger et al, *Nano Lett.* **2009**, *9*, 3066.

IV. Biological imaging and theranostics

A. Resonant light scattering: Darkfield microscopy

Plasmon-resonant NPs used as biological imaging labels must also compete with other scatterers.

Cross-polarized scattering: a novel method of noise reduction for anisotropic NP labels

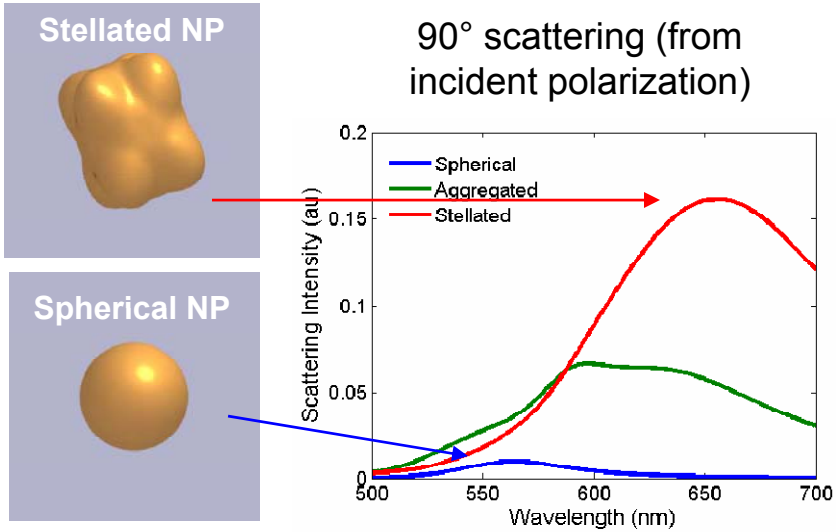

Aaron et al, *Opt. Express* **2008**, *16*, 2153.

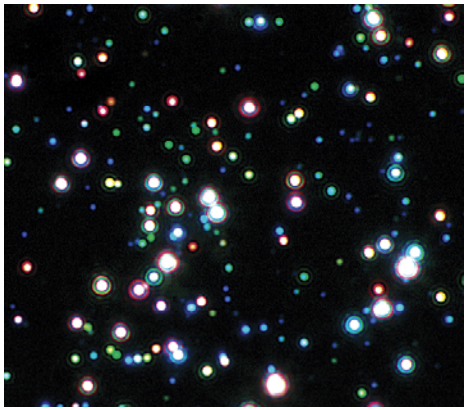

Ag nanoparticles of variable size and shape

A431 cells with anti-EGFR labeled nanostars

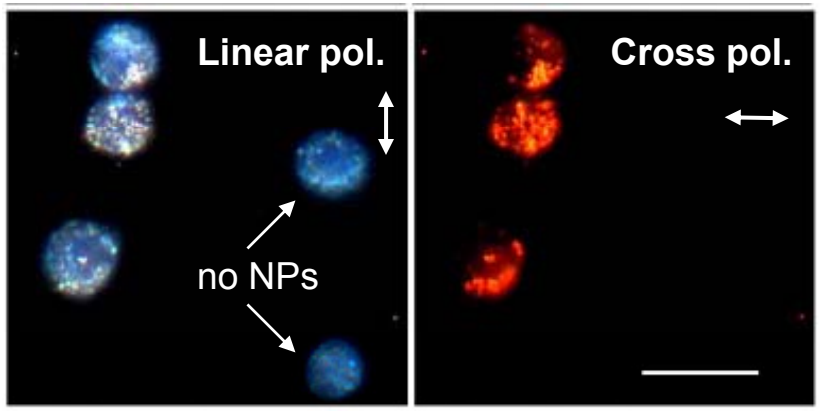

Au particles as dynamic imaging labels

Gyromagnetic imaging using Au nanostars with magnetic cores

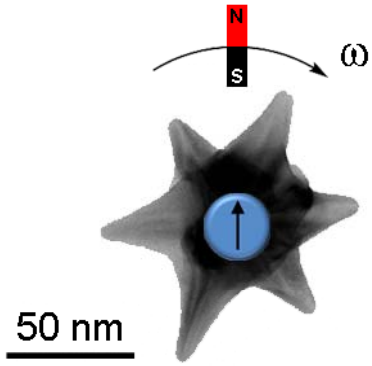

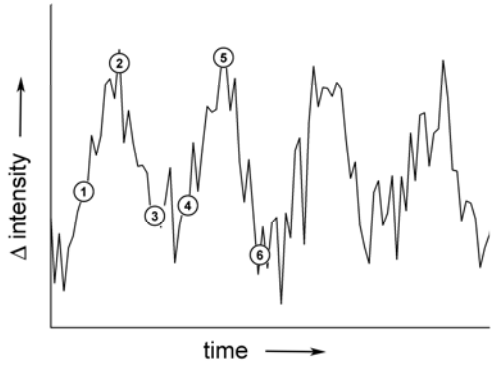

polarized scattering from single nanostar (in real time)

FFT

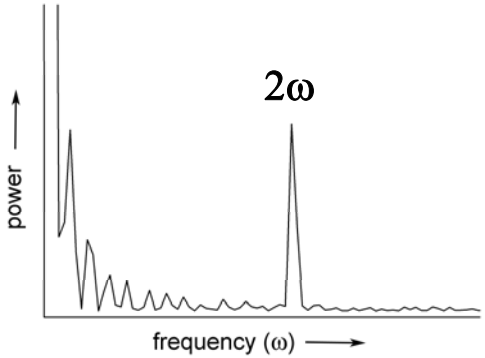

Power density spectrum with freq.-selective signal at 2ω

Nanostars in KB cell: frequency-selective filtering for noise reduction

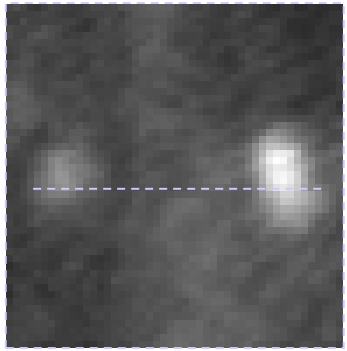

Time-domain (left signal): **15.9 dB**

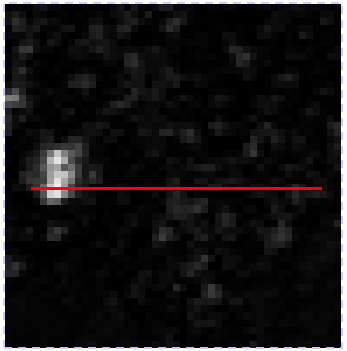

Fourier-domain signal: **28.1 dB**

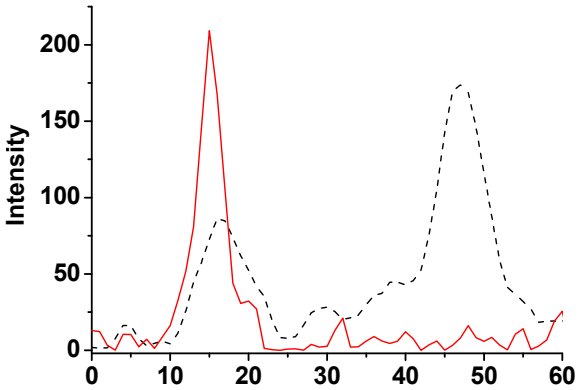

Wei et al, *J. Am. Chem. Soc.* **2009**, *131*, 9728.

B. Contrast agents for biomedical imaging

Optical coherence tomography (OCT)

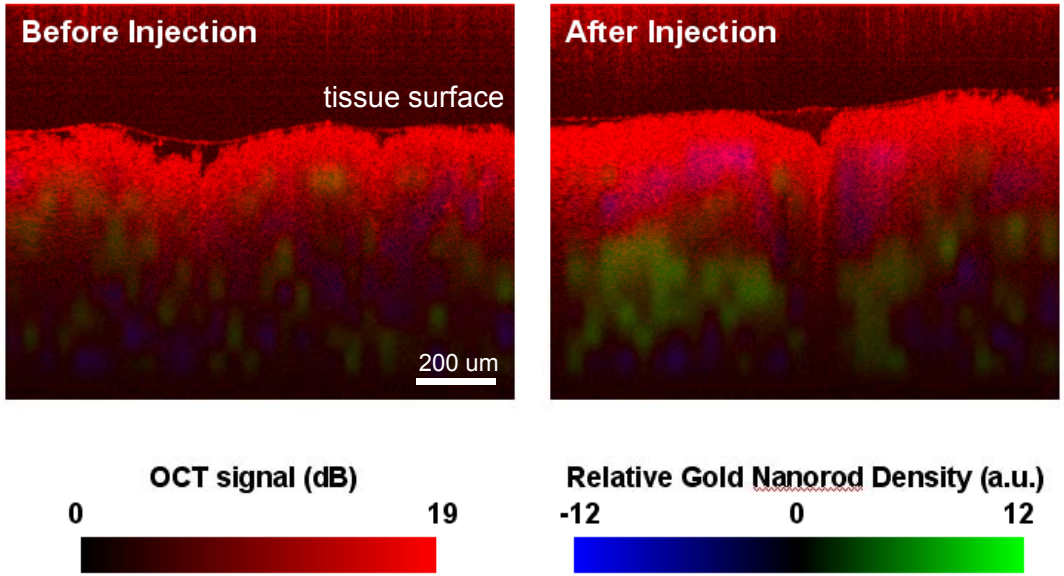

OCT contrast by Au NRs in human breast carcinoma tissue

Oldenburg et al, *J. Mater. Chem.* **2009**, *19*, 6407.

Eghtedari et al, *Nano Lett.* **2007**,*7*, 1914.

Photoacoustic tomography

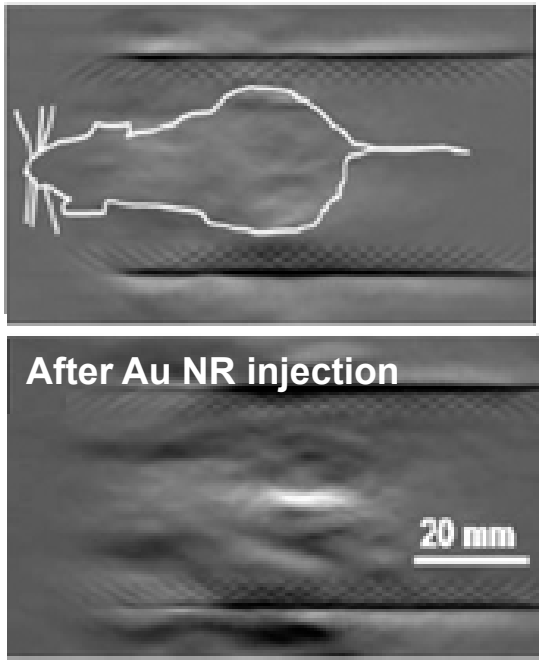

PAT of Au NRs within nude mouse (before and after injection)

Relatively high loadings of Au NPs are still required to generate sufficient contrast in tissue for these imaging modalities.

C. Nanoparticles as SERS tags

***in vitro* detection of antibody-labeled SERS tags: compares well with fluorescence imaging**

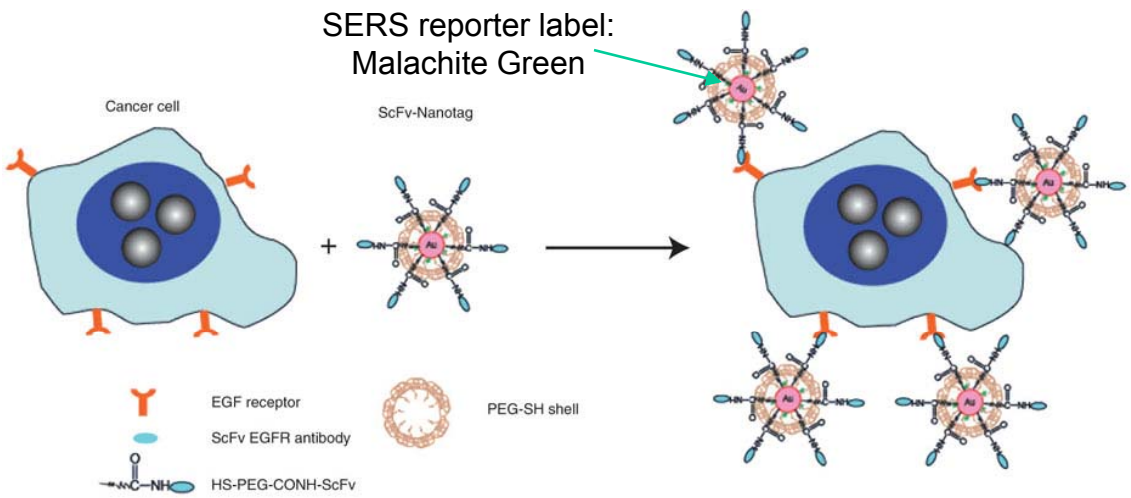

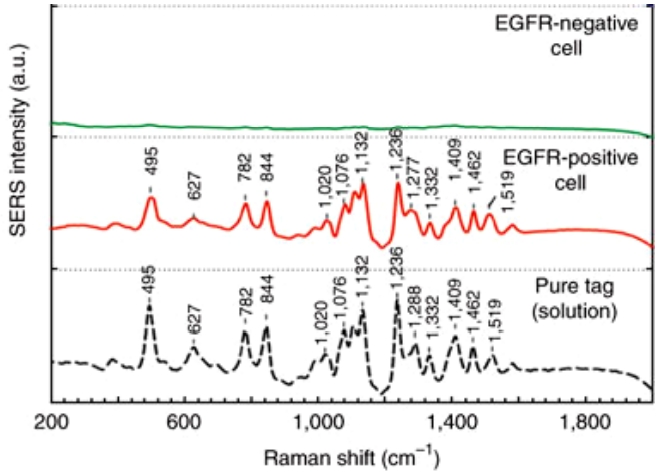

Targeted *in vivo* delivery of SERS labels to tumor in nude mouse model:

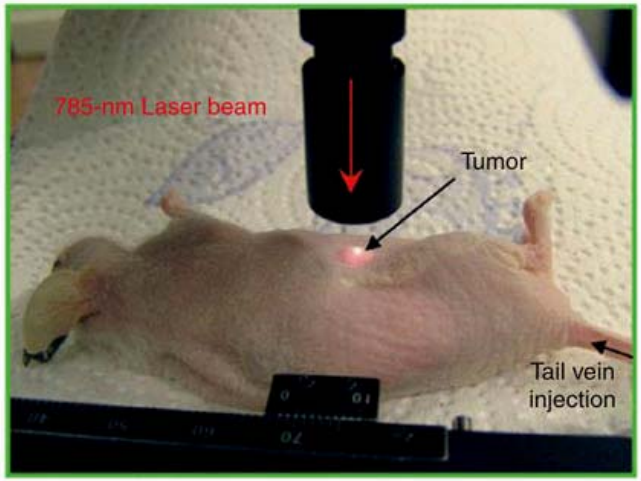

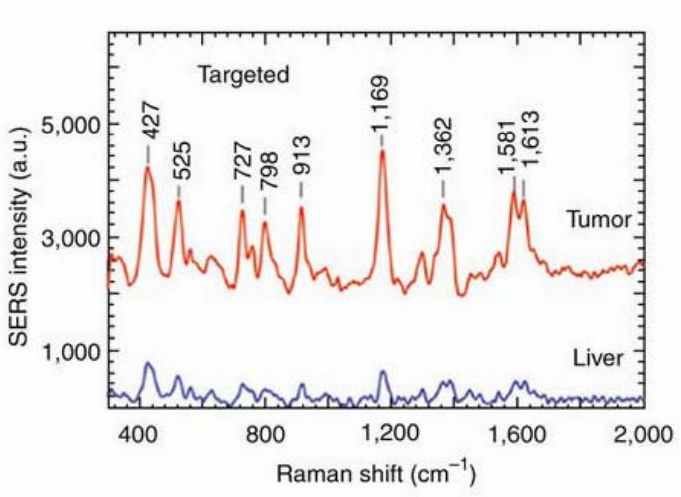

Qian et al, *Nat. Biotechnol.* **2008**, *26*, 83.

SERS imaging of biological events

Cell-surface receptor clustering: actuation of SERS signals

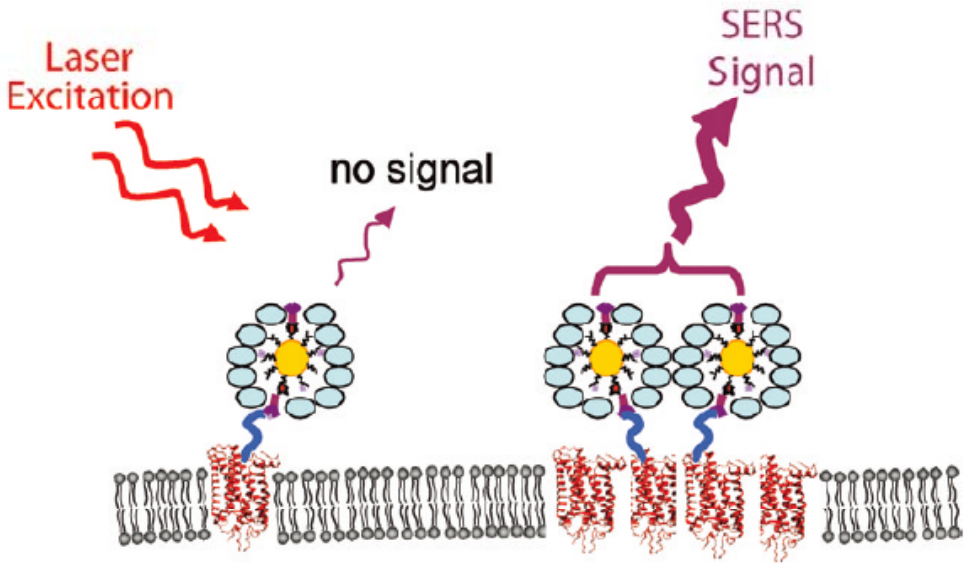

Receptor-mediated aggregation of Ag NPs, to monitor adrenergic signaling during the contraction of cardiac myocytes

Kennedy et al, *ACS Nano* **2009**, *3*, 2329

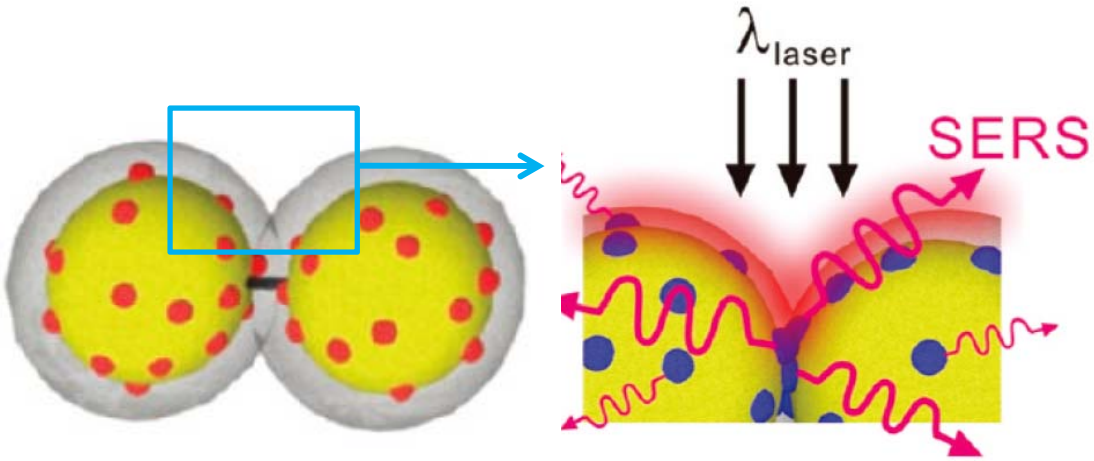

Silica or polymer-coated NPs with embedded SERS tags, functionalized with capture ligands (for cluster formation of cell surface)

Kennedy et al, *Chem. Commun.* **2009**, 6750

D. Multiphoton imaging

Two-photon excited luminescence (TPL) from Au nanorods (NRs)

Au nanorods

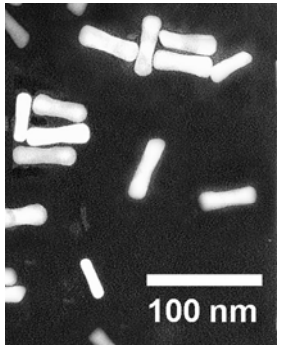

***sp*-hole relaxation after 2-photon abs.**

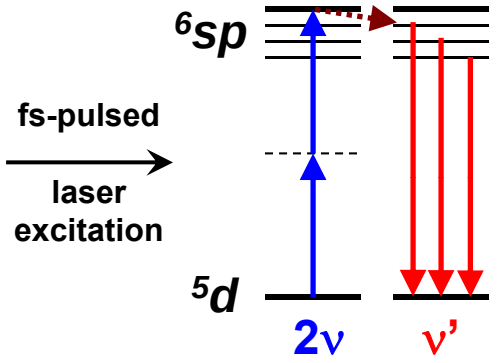

TPL of Au NRs on glass slide

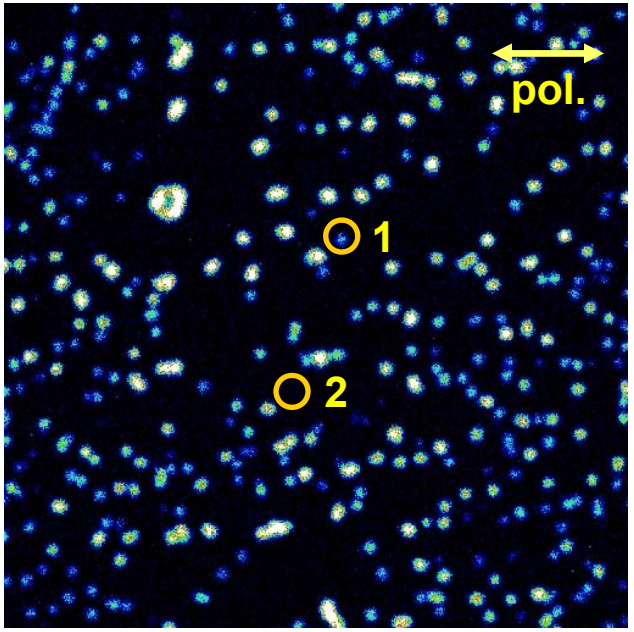

TPL intensity vs. Au NR absorption:

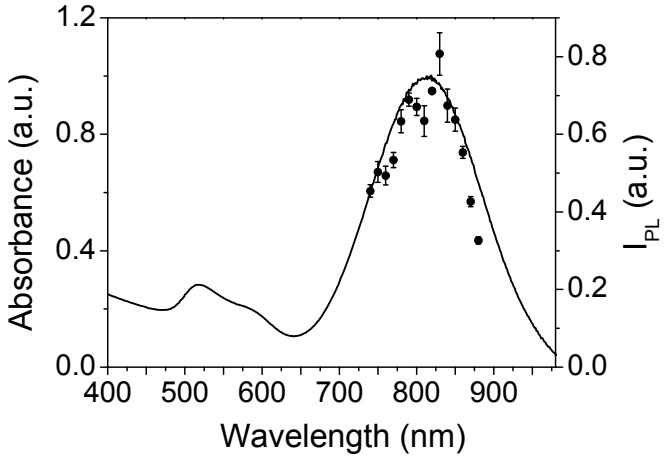

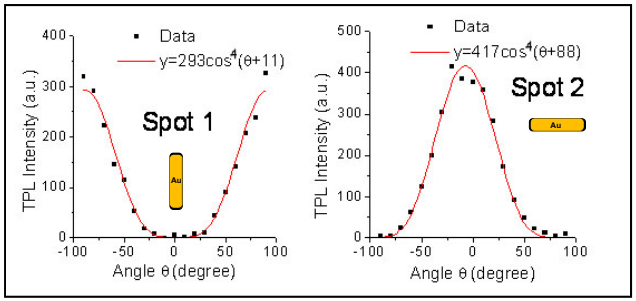

Wang *et al*. *PNAS* **2005**, *102*, 15752.

TPL imaging: extremely low autofluorescence

In vitro TPL imaging of Au NR uptake by KB cell: single-particle sensitivity

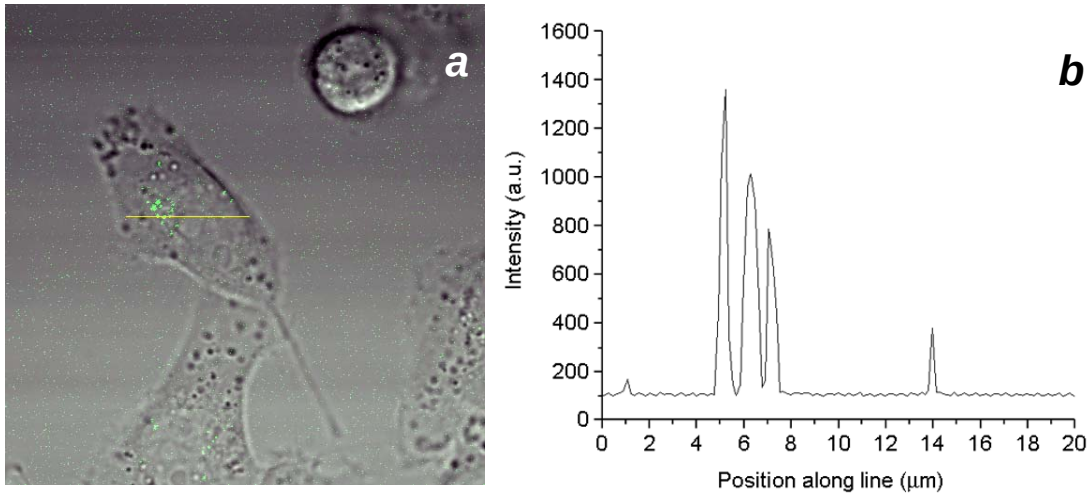

(a) TPL image of Au NRs (green) internalized by KB cells after a 5-hour incubation (linescan = 75 μm).

(b) Intensity profile across yellow linescan in (a); high SNR provided by TPL contrast.

Huff et al, *Nanomedicine* **2007**, *2*, 105.

In vivo TPL imaging of Au NRs flowing through blood vessel in mouse ear

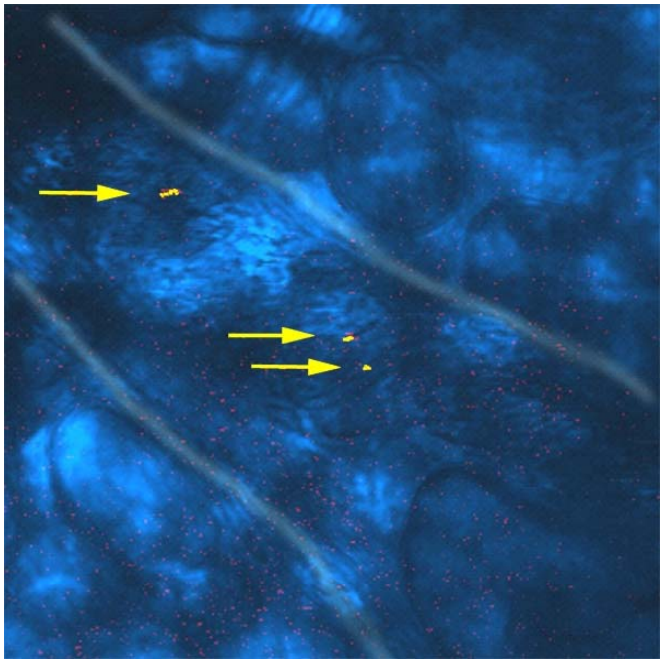

Wang *et al*. *PNAS* **2005**, *102*, 15752.

E. Photothermal activity of metal nanoparticles

Absorbed light is mostly converted into heat

Estimation of surface temperature on Au NP:

$$\Delta T = \frac{E_{abs}}{mc_p}$$

ΔT for 5-nm Au sphere =15 K at LSPR saturation

E_{abs} =absorbed photon energy
m =mass of Au NP
c_p = heat capacity of Au

Estimation of heat transfer to environment of Au NP:

$$\Delta T(r) = \frac{V_{NP}Q}{4\pi k_0 r}$$

1/*r* dependence

V_{NP} = volume of NP
Q = heat of NP
k_0 = thermal conductivity of medium
r = distance from surface

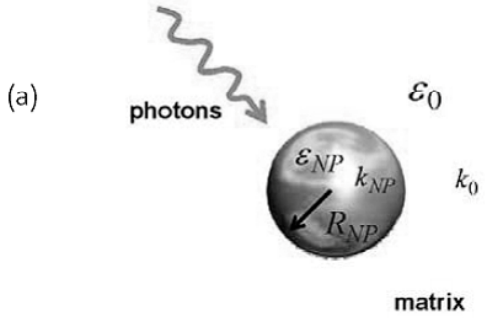

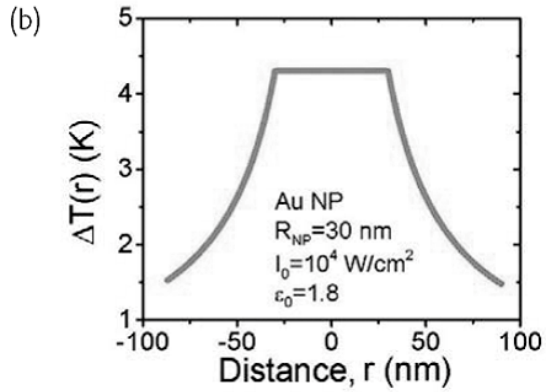

Govorov and Richardson, *Nano Today* **2007**, *2*, 30.

Site-dependent photothermolysis mediated by folate-conjugated Au NRs

Membrane-bound Au NRs on tumor cells

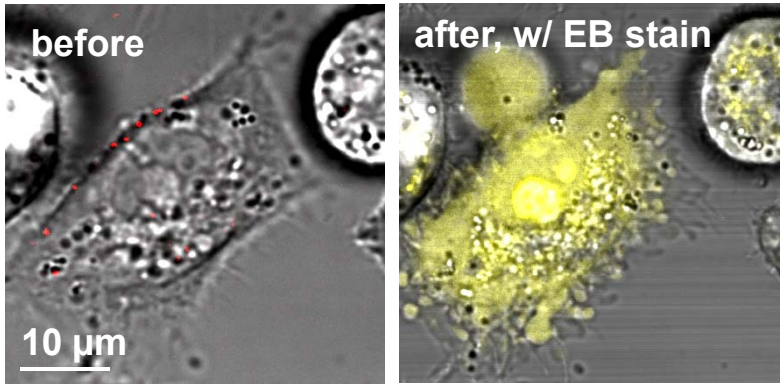

81 s scan, cw mode:
Laser power = 6 mw; fluence = 24 J/cm^2

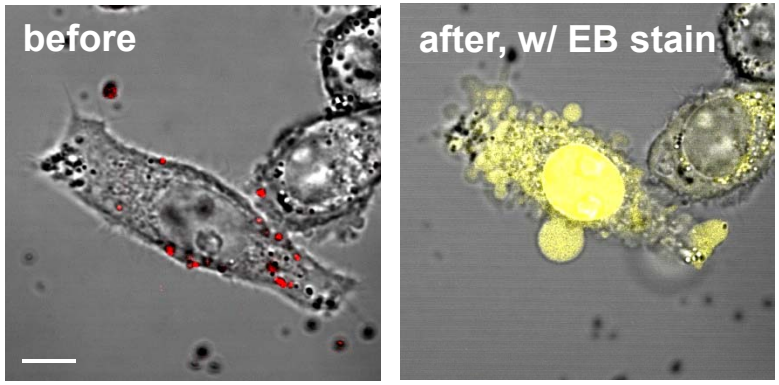

81 s scan, fs-pulsed mode:
Laser power = 0.75 mw; fluence = 3 J/cm^2

Internalized Au NRs

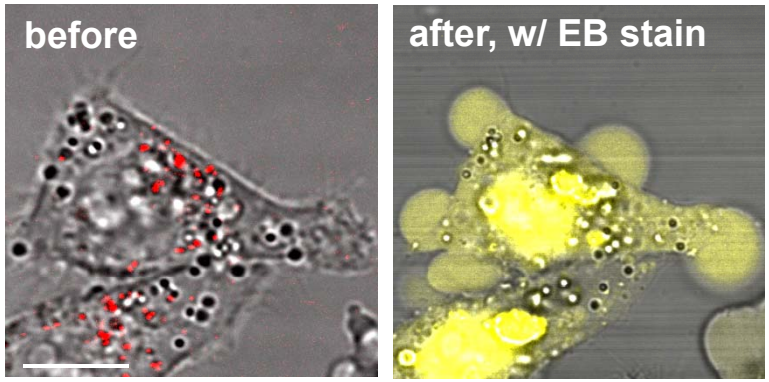

81 s scan, cw mode:
Laser power = 60 mw; fluence = 240 J/cm^2

Threshold fluence for hyperthermic damage (blebbing) is 10X lower or more when nanorods are localized on cell membranes

Tong et al, *Adv. Mater*. **2007** *19*, 3136.

Real-time imaging of nanorod-mediated membrane blebbing in KB cells

TPL excitation conditions:

λ_{ex} = 765 nm, 200-fs pulses, 77 MHz, 0.75 mW @ sample

Blebs are proximal and distal to membrane-bound nanorods

Tong et al, *Adv. Mater*. **2007** *19*, 3136.

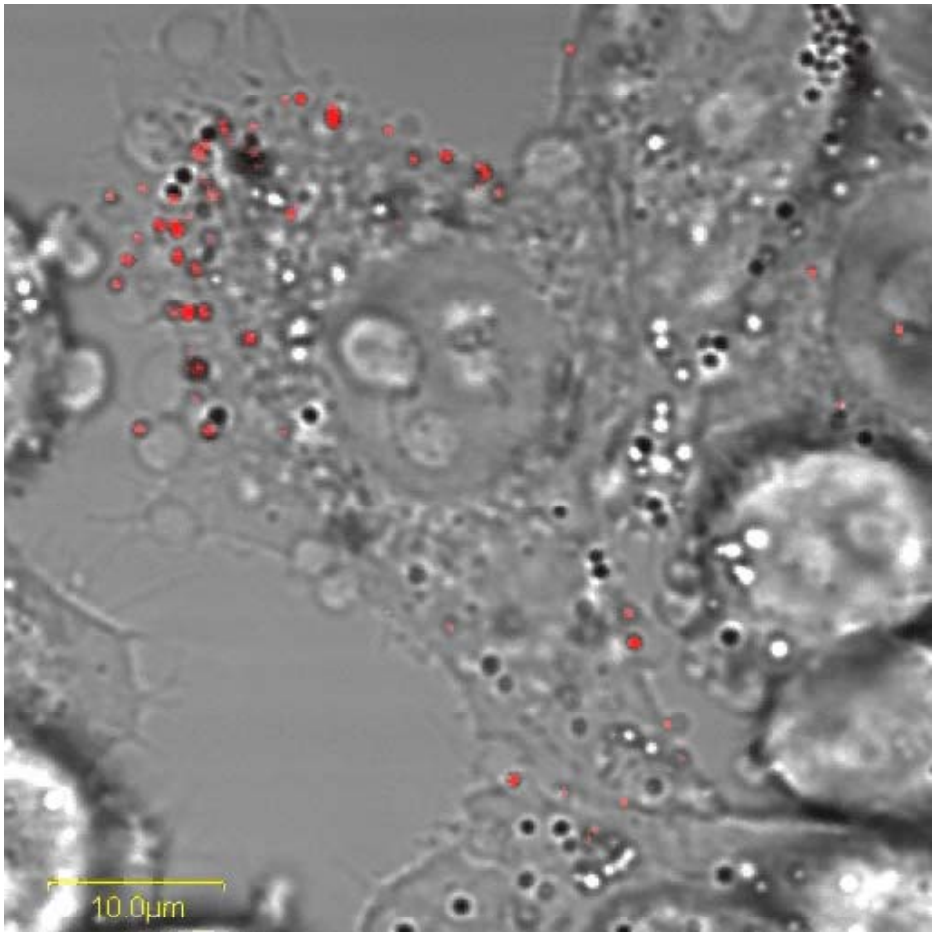

Timescale of photothermal response

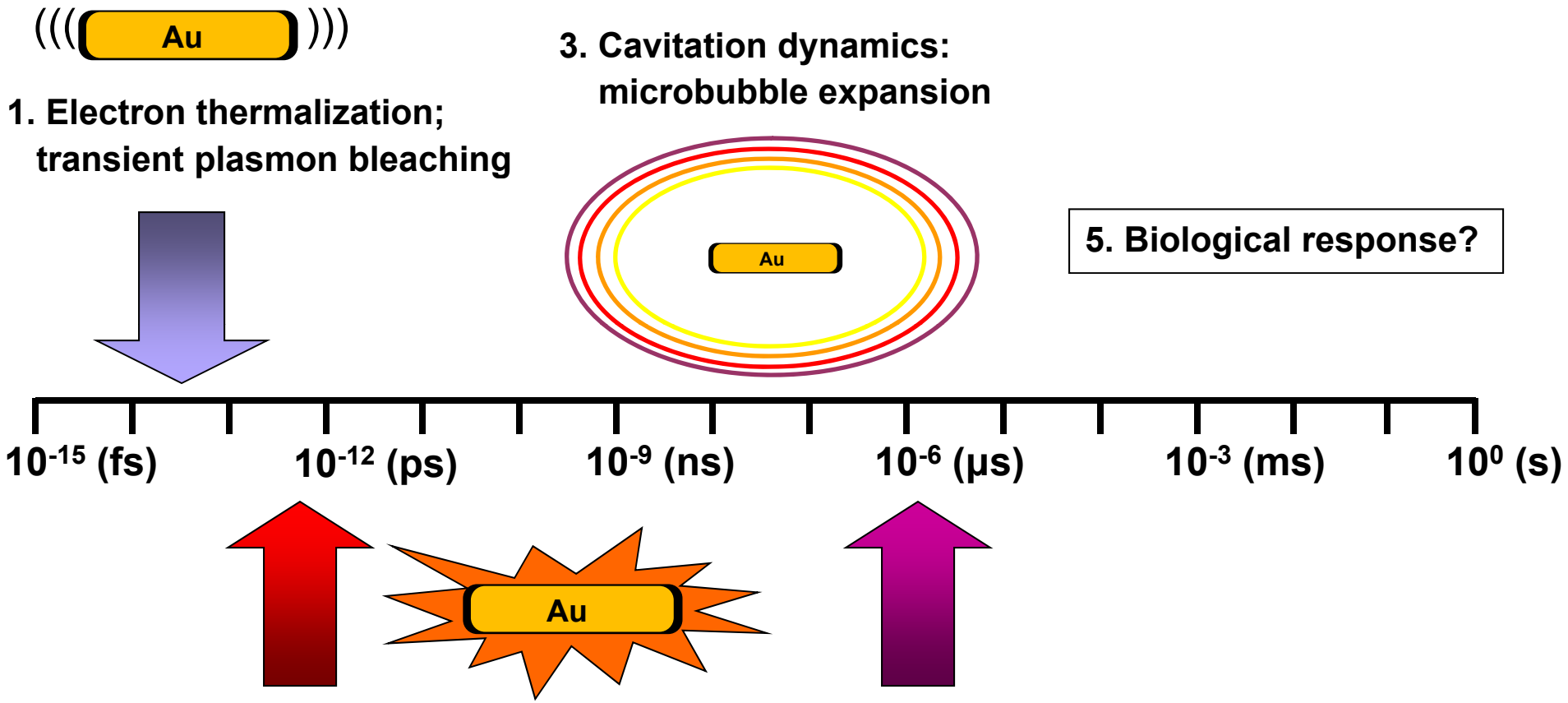

Link and El-Sayed, *Int. Rev. Phys. Chem.* **2000**, *19*, 409.
Pitsillides et al, *Biophys. J.* **2003**, *84*, 4023.

Nanorod-mediated membrane blebbing is due to extracellular Ca^{2+} influx

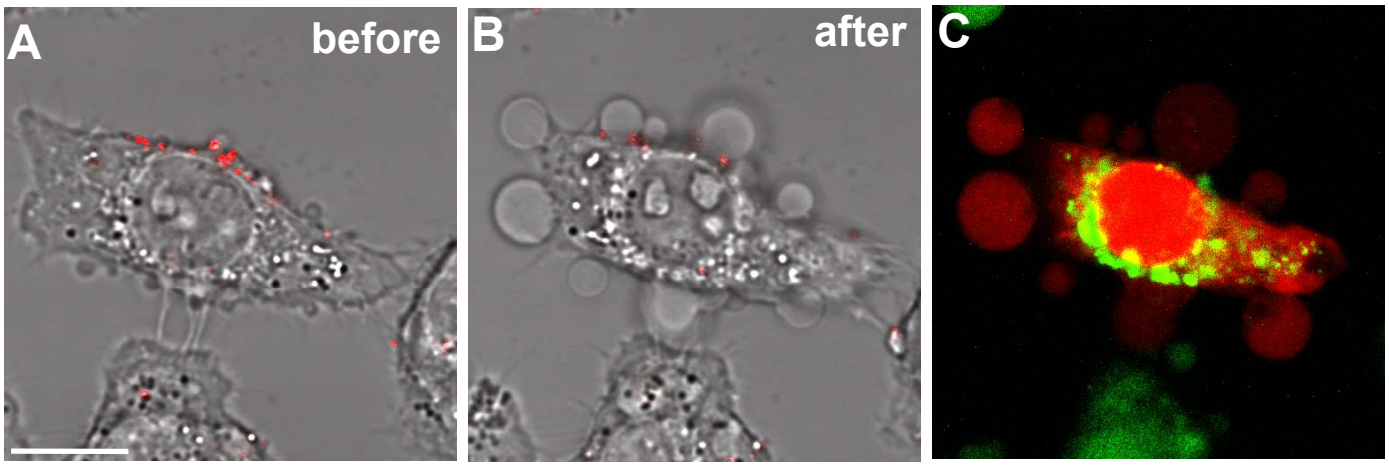

(A,B) KB cells with membrane-bound Au NRs (red) in media containing 0.9 mM Ca^{2+} (100 mg/L $CaCl_2$) exhibited blebbing after exposure to fs-pulsed laser irradiation at 3 mW for 61.5 s.

(C) Incubation with 2.5 μM EB (red) and 2 μM Oregon Green 488 for 20 min indicated a compromise in membrane integrity and an elevation in intracellular Ca^{2+}, respectively.

Tong et al, *Adv. Mater*. **2007** *19*, 3136.

Concluding remarks

- LSPRs are easily tuned as a function of particle size, shape, and surface dielectric for absorption or scattering at visible to NIR wavelengths

- Surface functionalization methods should ensure good dispersion control and be resistant against desorption under physiological conditions

- Plasmon-resonant NPs can support a variety of *in vitro* optical sensing and imaging modalities, often with single-particle sensitivity

- For *in vivo* imaging, new methods of signal generation and noise reduction are still needed in order to maintain low particle loadings into tissue

- Optical imaging of metal NPs can be coupled with a strong photothermal response, integrating diagnostics with therapeutic potential.

Acknowledgment of financial support from NIH (RC1 CA147096-01).